

# Support Tokens, Stability Margins, and a New Foundation for Robust LLMs

Deepak Agarwal<sup>1</sup>, Dhyey Dharmendrakumar Mavani<sup>1</sup>, Suyash Gupta<sup>1</sup>, Karthik Sethuraman<sup>1</sup>, and Tejas Dharamsi<sup>1</sup>

<sup>1</sup>LinkedIn, Mountain View, CA

<sup>1</sup>{dagarwal, dmavani, suyagupta, ksethuraman, tdharamsi}@linkedin.com

March 3, 2026

## Abstract

Self-attention is usually described as a flexible, content-adaptive way to mix a token with information from its past. We re-interpret causal self-attention transformers, the backbone of modern foundation models, within a probabilistic framework, much like how classical PCA is extended to probabilistic PCA. However, this re-formulation reveals a *surprising* and deeper structural insight: due to a change-of-variables phenomenon, a barrier constraint emerges on the self-attention parameters. This induces a highly structured geometry on the token space, providing theoretical insights into the dynamics of LLM decoding. This reveals a boundary where attention becomes ill-conditioned, leading to a *margin* interpretation similar to classical support vector machines. Analogous to support vectors, this naturally gives rise to the concept of *support tokens*.

Furthermore, we show that LLMs define a consistent stochastic process over (infinite) token sequences, providing a rigorous probabilistic framework for sequence modeling. We propose a Bayesian framework and derive a MAP estimation objective that requires only a minimal modification to standard LLM training: the addition of a smooth log-barrier penalty to the usual cross-entropy loss. We demonstrate that this provides more robust models without sacrificing out-of-sample accuracy and that it is straightforward to incorporate in practice.

**Keywords** Large Language Models · Robustness · Causal Attention · Large Margins · Stochastic Processes · Bayesian prior · MAP · Jacobian · Probabilistic Models

## 1 Introduction

Transformers are the default architecture for sequence modeling across language, vision, and beyond (Vaswani et al., 2017; Brown et al., 2020; Dosovitskiy et al., 2021). The heart of transformers is causal self-attention, which is often described as a content-adaptive weighted average: each token mixes information from its past according to similarity scores. Moving beyond this colloquial description, we ask a formal question:

*Does causal self-attention admit an explicit probabilistic interpretation, and if so, what does that interpretation imply about the geometry and inductive bias of the model?*

In this paper, we give a concrete answer. We show that causal self-attention can be interpreted as a probabilistic model on embeddings (treated as latent variables). A key consequence is a barrier constraint on the parameters of self-attention that emerges through this

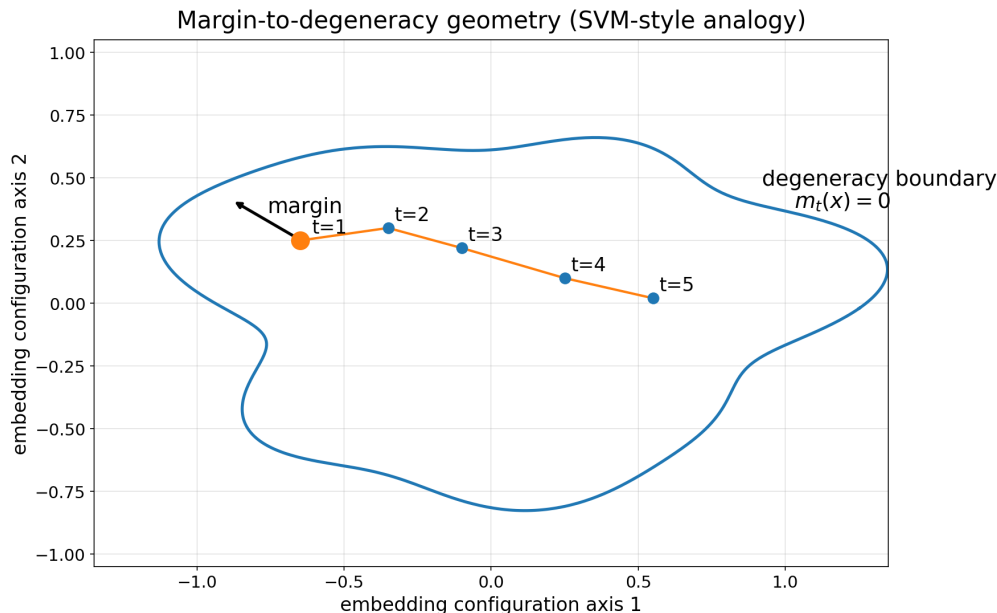


Figure 1.1: **Margin-to-degeneracy geometry (SVM-style analogy)**. The curve denotes an *instability boundary*: configurations where the attention-induced latent-noise map becomes locally ill-conditioned (small perturbations can lead to ambiguous or disproportionate changes). A sequence traces a trajectory of embedding configurations across token positions (dots). The *margin* of a token is its distance to this boundary (arrow). In this schematic, **token 1 is the support token** because it has the smallest margin (it lies closest to instability), so it governs the sequence-level stability margin and dominates the barrier pressure. This mirrors SVMs, where support vectors are the points closest to the decision boundary and therefore determine the margin. (Precise definitions appear in Section 3.)

probabilistic formulation; this induces an interesting geometry that leads to key ramifications. It shows that there is a boundary in the latent space where the attention-induced mapping becomes locally ill-conditioned. This defines a *margin to degeneracy* — a novel quantitative measure we introduce of how far each position is from that unstable boundary. This, in turn, helps us understand which tokens matter the most (Figure 1.1). The stability of a sequence is governed by its margin across positions. Tokens whose contexts are closest to degeneracy become the bottlenecks that dominate the barrier signal, directly analogous to support vectors in large-margin classifiers (Cortes and Vapnik, 1995). Moreover, the sign of this stability functional creates both attractive and repulsive coupling behaviors in the attention mechanism: positive values encourage attention to cluster around similar tokens, whereas negative values spread attention across highly dispersed tokens. This sign-dependent attractive/repulsive behavior is reminiscent of classical spin-coupling phenomena in the Ising model (Ising, 1925).

The “support token” perspective provides an interpretable explanation for where the additional likelihood pressure concentrates and motivates a practical training lever: adding (or stably approximating) the barrier term yields a controllable tradeoff between data fit and geometric conditioning of attention, analogous to classical regularization paths in regression models (Tibshirani, 1996; Efron et al., 2004).

Practically, the probabilistic formulation yields an immediate optimization lens. We work in a Bayesian framework (Bishop, 2006; Murphy, 2012) where the usual transformer model

of tokens conditioned on embeddings is treated as log-likelihood and we compose it with a log-prior based on a probabilistic causal transformer we identify in this paper. Formulating the log-posterior and performing MAP estimation yields the familiar data-fit term alongside a barrier term that enforces geometric stability. This connects causal self-attention to classical constrained estimation (Boyd and Vandenberghe, 2004): maximizing the posterior is equivalent to optimizing a squared-error objective (at noise scale  $\sigma$ ) under implicit margin constraints that keep the attention mapping well-behaved.

Beyond the single-layer self-attention mechanism, we also clarify how depth composes. In particular, we show how deep transformers can be interpreted as a hierarchical probability model across layers, and that the induced token distributions are consistent across sequence lengths, defining a well-posed stochastic process over token sequences.

## Contributions.

1. **A probabilistic interpretation of causal self-attention.** We formalize a causal self-attention layer as a conditional probability model over latent embeddings, which in turn induces a joint probability law over token sequences with an exact likelihood.
2. **Margin to degeneracy and a stability-inducing log-barrier.** We show that the induced likelihood contains an additional term that defines a margin to a critical degeneracy boundary and yields a smooth barrier against locally unstable attention geometries (Theorem 1).
3. **Optimization view.** We show that the log-likelihood can be written as a squared-error objective at noise scale  $\sigma$  together with a margin-based barrier term. Thus, our framework reinterprets existing transformers probabilistically rather than replacing them with a different model.
4. **A model-implied training penalty and empirical evidence.** Using a Bayesian formulation and MAP estimation (Bishop, 2006; Murphy, 2012), we derive a training penalty induced directly by the probabilistic model. This penalty requires no architectural modification and can be added to standard LLM training objectives; in our experiments, it improves robustness of the trained model.
5. **Depth as a hierarchy of conditional priors.** We characterize how the probabilistic interpretation composes across depth and identify conditions under which the nontrivial volume correction localizes to the first layer under standard transformer conditioning. This explains why a one-layer probabilistic causal prior is already a natural practical choice in the Bayesian setting.

**Organization.** Section 2 introduces our latent-noise view of causal self-attention as a structural (graphical) model over embeddings. Section 3 develops the single-layer theory and derives the margin/log-barrier term induced by token-dependent attention. Section 4 revisits these results from an optimization perspective, connecting the probabilistic objective to a squared-error formulation with a stability constraint, and clarifies the resulting training objective. Section 5 establishes that the induced family of token distributions is consistent across sequence lengths (i.e., defines a well-posed stochastic process), which is the key technical ingredient for learning from datasets of variable-length sequences. Section 6 extends the interpretation to depth, showing how layers compose into a hierarchy of conditional priors and

how the correction terms behave under standard conditioning. Section 7 evaluates the resulting penalty empirically. Section 8 surveys related work, and Section 9 discusses implications and future directions. All proofs are deferred to the Appendix.

## 2 A Latent-Noise View of Causal Self-Attention

This section introduces the probabilistic object for causal self-attention that is the core of the paper. The goal is not to modify the transformer architecture, but to make explicit the distribution over the model’s *embeddings* (hidden states) that a causal self-attention layer implicitly defines when viewed as a generative mechanism.

Fix a sequence length  $L$  and an embedding dimension  $d$ . We write

$$x_{1:L} = (x_1, \dots, x_L), \quad x_t \in \mathbb{R}^d,$$

for the sequence of continuous embeddings (hidden states) produced by a transformer (Vaswani et al., 2017; Brown et al., 2020). When we need to refer to depth, we write  $x_t^{(\ell)}$  for the layer- $\ell$  embedding, with  $x_t^{(0)}$  the input token embedding. We assume, without loss of generality for this discussion, that the embeddings are detrended, as the analysis applies equally to residuals. For clarity, we omit the layer index ( $\ell$ ) in sections focusing on the single-layer setting.

The transformer ultimately is used to define a probability model over discrete tokens via cross-entropy loss, but its computation proceeds through these continuous embeddings. Our focus in this paper is: *what probabilistic structure does causal self-attention induce over the embedding sequence  $x_{1:L}$ ?*

We adopt a probabilistic perspective: we treat embeddings as *random variables* rather than fixed activations. Concretely, we posit that embeddings are generated sequentially from latent noise,

$$\varepsilon_{1:L} = (\varepsilon_1, \dots, \varepsilon_L), \quad \varepsilon_t \in \mathbb{R}^d,$$

through a causal transformation. This is the same conceptual step that turns deterministic estimators into probabilistic models (e.g., probabilistic PCA (Tipping and Bishop, 1999), see also standard latent-variable modeling treatments (Bishop, 2006; Murphy, 2012)).

Throughout the main text we will use an isotropic Gaussian base noise,

$$\varepsilon_t \sim \mathcal{N}(0, \sigma^2 I_d), \tag{1}$$

where  $\sigma > 0$  controls the noise scale. In the limit  $\sigma \rightarrow 0$ , the usual deterministic view is recovered; at finite  $\sigma$ , the probabilistic formulation reveals additional geometric structure.

### 2.1 Causal self-attention as a probabilistic model over embeddings

Consider a single self-attention layer. For clarity, we start with a single head and write the usual query/key/value projections

$$q_t = W_Q x_t, \quad k_s = W_K x_s, \quad v_s = W_V x_s.$$

Causal self-attention forms a context summary  $\mu_t$  by attending to the past. In the *strict causal* form, (Vaswani et al., 2017; Brown et al., 2020)

$$\alpha_{ts}(x) = \frac{\exp(q_t^\top k_s)}{\sum_{r < t} \exp(q_t^\top k_r)}, \quad s < t, \quad \mu_t(x) = \sum_{s < t} \alpha_{ts}(x) v_s. \tag{2}$$

The standard deterministic view treats  $\mu_t$  as an update computed from the current embedding. Our probabilistic view instead treats  $\mu_t$  as the *mean* of a probability model for  $x_t$  given its context, with additive latent noise:

$$x_t = \mu_t(x) + \varepsilon_t, \quad \varepsilon_t \sim \mathcal{N}(0, \sigma^2 I_d). \quad (3)$$

The key modeling point is that  $\mu_t(x)$  is both *causal* (it uses only earlier positions) and *token-dependent*: the weights  $\alpha_{ts}(x)$  depend on the current token through the query  $q_t = W_Q x_t$ .

It is convenient to write (3) in residual form:

$$\varepsilon_t = e_t(x) \triangleq x_t - \mu_t(x). \quad (4)$$

This defines a transformation between latent variables  $\varepsilon_{1:L}$  and embeddings  $x_{1:L}$ , and it is this transformation that we analyze throughout the paper.

**Remark** Standard “causal” transformer implementations often include the current position in the context (i.e., they allow  $s \leq t$ ) (Radford et al., 2019; Brown et al., 2020), which introduces a nonzero self-weight  $\alpha_{tt}$  and a self-value term  $v_t$  inside  $\mu_t$ . Our main results and interpretations do not hinge on excluding  $s = t$ : the same token-dependent mechanism remains, and the induced likelihood still acquires an additional stability/conditioning term. We present the strict-causal setup (2) in the main text because it yields the cleanest exposition (and a directly auto-regressive interpretation). The modifications for  $s \leq t$  are straightforward and are stated in Appendix A.

## 2.2 The crucial log-Jacobian

Because  $\varepsilon_{1:L}$  has a tractable base density (1), the transformation (4) induces an explicit density over embeddings whenever it is locally invertible. The change-of-variables formula gives (Papamakarios et al., 2021)

$$\log p(x_{1:L}) = \log p(\varepsilon_{1:L}) + \log |\det J_{x \mapsto \varepsilon}(x_{1:L})|. \quad (5)$$

The first term is the familiar “noise energy” (a prediction-error term under the Gaussian choice). The second term is the crucial one: it accounts for local volume change under the attention-induced transformation.

Why does this term not vanish? Because attention is *token-dependent*. Even though  $\mu_t$  summarizes the past, the weights used to summarize it depend on the current token through  $q_t = W_Q x_t$ . As a result, the residual map  $e_t(x) = x_t - \mu_t(x)$  is not simply “ $x_t$  minus a past-only average”; it is a token-dependent reparameterization that generically induces a nontrivial volume factor in the exact likelihood.

In the next section we compute this volume factor explicitly and show that it defines a *margin to degeneracy*: it quantifies how far the attention-induced map is from a critical surface where it becomes locally singular. This yields a smooth barrier-like term in the log-likelihood that shapes attention geometry in a principled way.

## 3 Single-Layer Geometry: Margin and the Context-Dispersion Penalty

This section makes the probabilistic interpretation concrete for the simplest nontrivial object: a *single* causal self-attention layer viewed as a latent-noise generator of embeddings. The key

takeaway is that token-dependent attention induces an *additional* term for the log-probability density that diverges to  $-\infty$  near a degeneracy boundary (where it becomes locally singular), thus behaving like a smooth *log-barrier* (Boyd and Vandenberghe, 2004) that disfavors unstable configurations. We derive this effect in the scalar case ( $d = 1$ ), where the geometry is transparent, and then state the general  $d > 1$  result, where scalar variance becomes an attention-weighted covariance matrix. All proofs are deferred to Appendix B.

We work with the latent-noise formulation from Section 2. A single strict-causal self-attention layer defines a context summary  $\mu_t(x)$  from the past, and we study the induced residual map

$$\varepsilon_t = e_t(x) \triangleq x_t - \mu_t(x), \quad (6)$$

under a tractable base density on  $\varepsilon_{1:L}$  (here  $\varepsilon_t \sim \mathcal{N}(0, \sigma^2 I_d)$ ). The crucial point is that  $\mu_t(x)$  depends on  $x_t$  through the query, so  $x \mapsto \varepsilon$  is a token-dependent transformation; its local sensitivity depends on the configuration of the attended context.

### 3.1 Simple case: the scalar ( $d = 1$ )

We begin with  $d = 1$ , so  $x_t, v_s \in \mathbb{R}$ . Let  $\alpha_{ts}$  denote the strict-causal attention weights, and define the attention-weighted mean and variance of the attended values:

$$\bar{v}_t \triangleq \sum_{s < t} \alpha_{ts} v_s, \quad \text{Var}_t \triangleq \sum_{s < t} \alpha_{ts} (v_s - \bar{v}_t)^2. \quad (7)$$

Because  $\alpha_{ts}$  depends on the current token through  $q_t = W_Q x_t$ , the residual map  $e_t(x) = x_t - \mu_t(x)$  has a nontrivial diagonal derivative.

**Proposition 1** (Scalar diagonal derivative). *Assume  $d = 1$  and bilinear logits  $q_t^\top k_s$  with  $q_t = W_Q x_t$  and  $k_s = W_K x_s$ . Then for each  $t$ ,*

$$\frac{\partial e_t}{\partial x_t} = 1 - a \text{Var}_t, \quad a \triangleq W_K W_Q. \quad (8)$$

Equation (8) already captures the central phenomenon: the local sensitivity of the map  $x_t \mapsto \varepsilon_t$  is governed by the attention-weighted dispersion of the attended context. Importantly, the coefficient  $a$  can have either sign, so the way dispersion affects sensitivity depends on the effective query-key parameterization; what is universal is that the map becomes unstable when the derivative approaches zero.

### 3.2 Margin to degeneracy and “support tokens”

Proposition 1 motivates defining a position-wise *margin to degeneracy*:

$$m_t(x) \triangleq 1 - a \text{Var}_t(x). \quad (9)$$

The attention-induced map becomes locally singular at position  $t$  precisely when  $m_t(x) = 0$ , i.e., when  $\partial e_t / \partial x_t = 0$ . This defines a *degeneracy boundary* (a critical surface) in embedding space.

To summarize stability across the whole sequence, we define the *sequence margin*

$$m(x) \triangleq \min_{t \in \{1, \dots, L\}} m_t(x). \quad (10)$$

Indices attaining (or nearly attaining) this minimum are the bottlenecks for stability.

**Definition 3.1** (Support tokens). *Any index  $t^* \in \arg \min_t m_t(x)$  is called a support token. These are the positions whose attention geometry lies closest to the degeneracy boundary and therefore most strongly constrains the global margin.*

This is directly reminiscent of large-margin classifiers, where a small subset of points (support vectors) controls the margin (Cortes and Vapnik, 1995). Here, support tokens are the positions that dominate the stability pressure induced by the probability distribution.

### 3.3 Decomposition of log-density and the log-barrier term

Assume we are in a locally invertible regime where  $m_t(x) \neq 0$  for all  $t$  (and in particular, for the simplest “stable” case,  $m_t(x) > 0$ ). Under the Gaussian noise model  $\varepsilon_t \sim \mathcal{N}(0, \sigma^2)$ , the change-of-variables formula (Papamakarios et al., 2021) yields the induced log-density over embeddings:

$$\log p(x_{1:L}) = -\frac{1}{2\sigma^2} \sum_{t=1}^L e_t(x)^2 + \sum_{t=1}^L \log \left| \frac{\partial e_t}{\partial x_t} \right| - L \log \sigma + \text{const.} \quad (11)$$

Using Proposition 1, the additional term becomes

$$\sum_{t=1}^L \log |1 - a \text{Var}_t(x)| = \sum_{t=1}^L \log |m_t(x)|. \quad (12)$$

This is the *missing* term relative to a pure prediction-error objective. Its role is a smooth log-barrier: as any margin approaches the degeneracy boundary  $m_t(x) \rightarrow 0$ , we have  $\log |m_t(x)| \rightarrow -\infty$ , sharply down-weighting such configurations. Thus, the exact log-probability does not merely fit residuals; it also prefers attention geometries that keep the token-dependent map away from local singularities.

### 3.4 Theory illustration: positive vs. negative coupling in the scalar case

The scalar formula (8) already shows that the sign of the effective coupling  $a = W_K W_Q$  determines the qualitative behavior of the additional likelihood term. When  $a > 0$ , the margin

$$m_t(x) = 1 - a \text{Var}_t(x)$$

decreases with attention-weighted variance and can approach zero, producing a true log-barrier against degeneracy. When  $a < 0$ , the same factor becomes  $1 + |a| \text{Var}_t(x)$ , which stays strictly positive: the singular boundary disappears, and the change-of-variables term instead amplifies configurations with larger dispersion rather than excluding them.

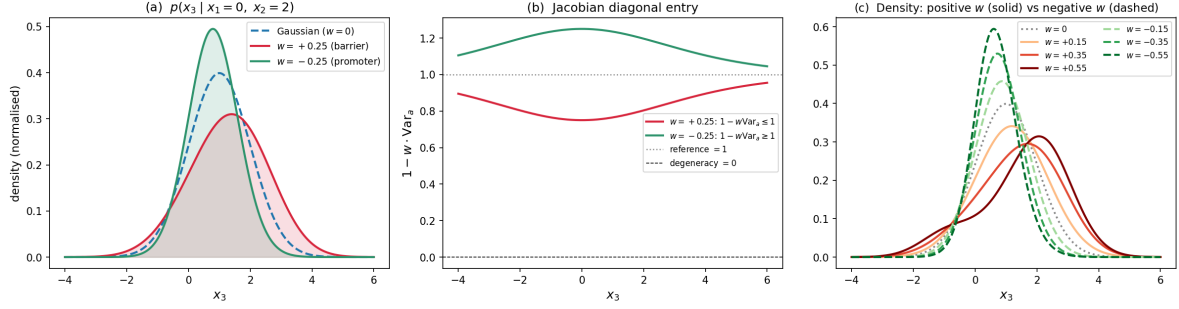


**Figure 3.2: Prior density under positive and negative coupling ( $d=1, n=3$ ).** (a) Conditional density of  $x_3$  given  $x_1=0, x_2=2$ . Positive coupling ( $a=+0.25$ , red) lowers and broadens the peak (from  $\approx 0.38$  for the Gaussian baseline to  $\approx 0.32$ ) because the change-of-variables factor  $1 - a \text{Var}_a < 1$  reduces log-density at nonzero dispersion. Negative coupling ( $a=-0.25$ , green) sharpens the density and raises the peak to  $\approx 0.52$  because  $1 - a \text{Var}_a > 1$  amplifies the same region. (b) The diagonal factor  $1 - a \text{Var}_a$  (Eq. 8) as a function of  $x_3$ : for  $a > 0$  it decreases toward the degeneracy boundary ( $\approx 0.75$  here, reaching 0 at  $\text{Var}_a = 1/a$ ), while for  $a < 0$  it increases above 1 (to  $\approx 1.25$  here) and remains strictly nondegenerate. (c) Density profiles for  $a \in \{-0.55, -0.35, 0, +0.35, +0.55\}$ : larger positive coupling progressively flattens the density, whereas larger negative coupling progressively sharpens it.

$w > 0$  (barrier/penalty) vs  $w < 0$  (promoter/always-invertible)

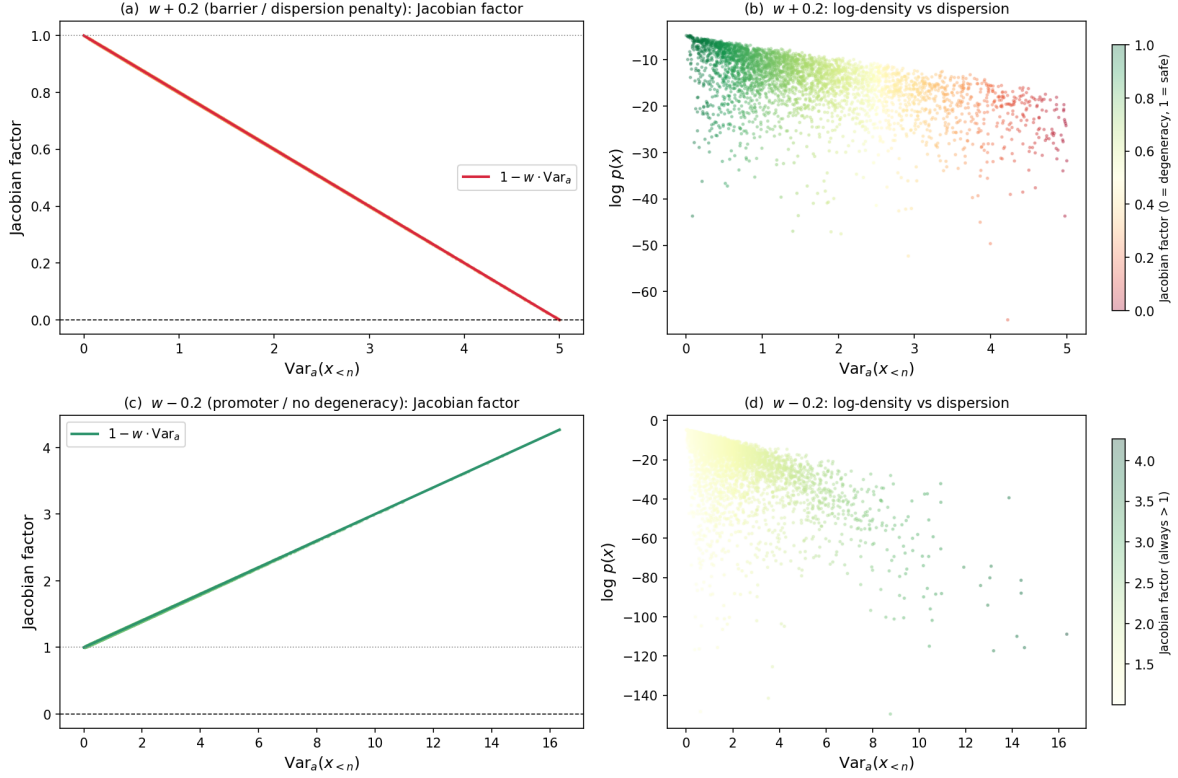


Figure 3.3: **Positive vs. negative coupling regimes** ( $d=1$ ,  $n=5$ ). 4000 random sequences from  $\mathcal{N}(0, 4)$  evaluated under positive coupling ( $a = +0.2$ , top row) and negative coupling ( $a = -0.2$ , bottom row). (a) For  $a > 0$ , the diagonal factor follows  $1 - a \text{Var}_a$  exactly, decreases linearly, and reaches 0 near  $\text{Var}_a \approx 5$ ; only 3387/4000 sequences remain valid. (b) For  $a > 0$ , log-density decreases with  $\text{Var}_a$ , and configurations near degeneracy are hard-excluded (red points, log-density =  $-\infty$ ). (c) For  $a < 0$ , the factor follows  $1 + |a| \text{Var}_a$ , increases linearly, and stays strictly above 1; all 4000/4000 sequences remain valid, and  $\text{Var}_a$  extends to  $\approx 16$ . (d) For  $a < 0$ , log-density still decreases overall because the Gaussian residual term dominates, but no sequence is excluded and the change-of-variables term partially offsets that decay (about  $+\log(4.2) \approx +1.4$  nats at  $\text{Var}_a = 16$ ). Together, the panels show that positive coupling induces a true degeneracy barrier, whereas negative coupling removes the barrier and instead promotes larger dispersion.

Figures 3.2 and 3.3 illustrate these two regimes in the simplest scalar setting. We fix  $x_1 = 0$ ,  $x_2 = 2$ , sweep  $x_3 \in [-4, 6]$ , and compare the induced conditional density under positive, zero, and negative coupling. We also evaluate 4000 random length-5 sequences to visualize the population-level relationship between  $\text{Var}_t$ , the diagonal factor, and the log-density.

Figure 3.2 shows the local effect on the conditional density. For positive coupling ( $a = +0.25$ ), the change-of-variables factor is less than one whenever  $\text{Var}_t > 0$ , so it subtracts from the log-density and flattens the peak: the maximum density drops from approximately 0.38 (Gaussian reference) to 0.32. For negative coupling ( $a = -0.25$ ), the factor is greater than one, so it adds to the log-density and sharpens the peak to approximately 0.52. As expected

from (8), the diagonal factor follows the exact linear form  $1 - a \text{Var}_t$ , and increasing  $|a|$  makes the deviation from the Gaussian more pronounced.

Figure 3.3 shows the corresponding population-level behavior. For positive coupling ( $a = +0.2$ ), the factor decreases linearly toward zero and 613 out of 4000 sequences (15.3%) are excluded by the degeneracy condition; among the remaining 3387 valid sequences, log-density decreases as  $\text{Var}_t$  increases. For negative coupling ( $a = -0.2$ ), all 4000 sequences remain valid, the diagonal factor increases as  $1 + |a| \text{Var}_t$ , and the observed range of  $\text{Var}_t$  extends to approximately 16 (compared with approximately 5 in the positive-coupling case). The log-density still decreases overall because the Gaussian residual term dominates in the tails, but the change-of-variables term now partially offsets that decay instead of imposing a hard barrier.

These illustrations make the sign dependence explicit: *positive coupling yields a genuine margin-to-degeneracy and a log-barrier, while negative coupling removes the degeneracy boundary and turns the same term into a dispersion-promoting correction.*

### 3.5 General case ( $d > 1$ ): covariance and a matrix margin

We now state the corresponding result in  $d > 1$ . Define the attention-weighted mean and covariance of the attended values:

$$\bar{v}_t \triangleq \sum_{s < t} \alpha_{ts}(x) v_s, \quad \Sigma_t \triangleq \sum_{s < t} \alpha_{ts}(x) (v_s - \bar{v}_t)(v_s - \bar{v}_t)^\top \succeq 0. \quad (13)$$

**Theorem 1** (Diagonal Jacobian block and conditioning). *For the residual map  $e_t(x) = x_t - \mu_t(x)$  induced by strict-causal self-attention (Section 2), the diagonal Jacobian block satisfies*

$$\frac{\partial e_t}{\partial x_t} = I_d - \Sigma_t A, \quad (14)$$

where  $A$  is an explicit matrix determined by the query/key parameterization. In the basic bilinear logit model with  $q_t = W_Q x_t$  and  $k_s = W_K x_s$ , one has

$$A = W_K^\top W_Q. \quad (15)$$

This identifies a natural matrix-valued notion of “distance to degeneracy”: the map becomes locally singular at  $t$  precisely when  $\det(I_d - \Sigma_t A) = 0$ . Equivalently, stability can be expressed via spectral conditions on  $\Sigma_t A$  (formalized in Appendix B.6).

**Corollary 3.1** (Log-likelihood and the context-geometry term). *Assume we are in a locally invertible regime where  $\det(I_d - \Sigma_t A) \neq 0$  for all  $t$ . Under  $\varepsilon_t \sim \mathcal{N}(0, \sigma^2 I_d)$ , the induced log-density over embeddings decomposes as*

$$\log p(x_{1:L}) = -\frac{1}{2\sigma^2} \sum_{t=1}^L \|e_t(x)\|_2^2 + \sum_{t=1}^L \log |\det(I_d - \Sigma_t A)| - Ld \log \sigma + \text{const}. \quad (16)$$

*The second term is the additional geometry/conditioning term induced by token-dependent attention: it diverges to  $-\infty$  as  $\det(I_d - \Sigma_t A) \rightarrow 0$ , acting as a smooth barrier against locally singular attention-induced transformations.*

## 4 An Optimization View: Squared Error Under a Stability Margin

The previous sections define an explicit probabilistic model over embedding sequences: latent noise  $\varepsilon_{1:L}$  is mapped to embeddings  $x_{1:L}$  through the token-dependent causal attention transformation, yielding an exact log-probability via change-of-variables (Papamakarios et al., 2021). This section takes an *optimization lens* on that likelihood. The key result is simple: *maximizing the embedding prior likelihood is equivalent to a squared-error objective (at noise scale  $\sigma$ ) together with a stability term that acts as a log-barrier against approaching the degeneracy boundary* (Boyd and Vandenberghe, 2004). We present the scalar case first, where the constraint has an explicit “margin” form, and then state the general  $d$ -dimensional counterpart.

Recall the latent-noise generative rule

$$x_t = \mu_t(x) + \varepsilon_t, \quad \varepsilon_t \sim \mathcal{N}(0, \sigma^2 I_d), \quad (17)$$

with residual map  $e_t(x) = x_t - \mu_t(x)$  and the induced embedding density (obtained by change-of-variables (Papamakarios et al., 2021))

$$\log p_\sigma(x_{1:L}) = -\frac{1}{2\sigma^2} \sum_{t=1}^L \|e_t(x)\|_2^2 + \sum_{t=1}^L \log \left| \det \left( \frac{\partial e_t}{\partial x_t} \right) \right| - Ld \log \sigma + \text{const}. \quad (18)$$

Here the first term is a familiar squared-error fit to the attention prediction  $\mu_t(x)$ , and the second term is the stability/conditioning correction induced by token-dependent attention (Section 3).

Maximizing  $\log p_\sigma(x_{1:L})$  is equivalent (up to additive constants and a scaling) to minimizing the negative log-likelihood:

$$\mathcal{L}_{\text{prior},\sigma}(x) \triangleq \frac{1}{2\sigma^2} \sum_{t=1}^L \|x_t - \mu_t(x)\|_2^2 - \sum_{t=1}^L \log \left| \det \left( \frac{\partial e_t}{\partial x_t} \right) \right|. \quad (19)$$

We interpret (19) as *squared error under a stability margin*: the first term encourages embeddings to be close to their attention-predicted contexts, while the second discourages configurations where the attention-induced mapping becomes ill-conditioned.

In the scalar case ( $d = 1$ ), Section 3 showed that

$$\frac{\partial e_t}{\partial x_t} = m_t(x) \triangleq 1 - a \text{Var}_t(x), \quad (20)$$

where  $\text{Var}_t$  is the attention-weighted variance of attended values and  $a = W_K W_Q$  is the scalar analogue of  $W_K^\top W_Q$ .

Substituting (20) into (19) yields a particularly transparent objective:

$$\mathcal{L}_{\text{prior},\sigma}(x) = \frac{1}{2\sigma^2} \sum_{t=1}^L (x_t - \mu_t(x))^2 - \sum_{t=1}^L \log |m_t(x)| \quad (+ \text{const}). \quad (21)$$

**Barrier interpretation.** The set  $\{x : m_t(x) = 0\}$  is the *degeneracy boundary* at position  $t$ : the residual map loses local invertibility there. Accordingly,  $-\log |m_t(x)|$  acts as a smooth barrier that grows without bound as  $m_t(x) \rightarrow 0$  (Boyd and Vandenberghe, 2004). In optimization terms, maximizing likelihood discourages sequences whose attention geometry pushes the map toward singularity.

**An explicit constrained form (“margin constraint”).** Equation (21) can be viewed as a softened constrained problem: for any target margin level  $\delta > 0$ , consider

$$\min_x \frac{1}{2\sigma^2} \sum_{t=1}^L (x_t - \mu_t(x))^2 \quad \text{s.t.} \quad m_t(x) \geq \delta \quad \forall t. \quad (22)$$

The log-barrier objective (21) is the classical interior-point relaxation of (22) (Boyd and Vandenberghe, 2004): it replaces hard constraints  $m_t(x) \geq \delta$  with a barrier that becomes large as  $m_t(x)$  approaches 0. This makes the “stability margin” viewpoint precise: likelihood maximization trades off data fit against maintaining a positive margin away from degeneracy.

For  $d > 1$ , Theorem 1 gives the diagonal block

$$\frac{\partial e_t}{\partial x_t} = I_d - \Sigma_t A, \quad A = W_K^\top W_Q, \quad (23)$$

with  $\Sigma_t$  the attention-weighted covariance of attended values. Substituting into (19) yields

$$\mathcal{L}_{\text{prior},\sigma}(x) = \frac{1}{2\sigma^2} \sum_{t=1}^L \|x_t - \mu_t(x)\|_2^2 - \sum_{t=1}^L \log |\det(I_d - \Sigma_t A)| \quad (+ \text{const}). \quad (24)$$

**Matrix margin.** The degeneracy boundary is characterized by  $\det(I_d - \Sigma_t A) = 0$ , i.e., by configurations where 1 becomes an eigenvalue of  $\Sigma_t A$ . This suggests a natural “margin to degeneracy” at each position, such as

$$m_t(x) \triangleq |\det(I_d - \Sigma_t A)| \quad \text{or} \quad m_t(x) \triangleq 1 - \rho(\Sigma_t A), \quad (25)$$

where  $\rho(\cdot)$  denotes the spectral radius. Different choices are useful in different analyses; the log-likelihood itself selects the log-determinant form in (24).

#### 4.1 Integration into the full token model

So far we have focused on the embedding prior  $p_\sigma(x_{1:L})$  induced by causal attention. To model actual token sequences  $y_{1:L}$ , we will combine this prior with the standard transformer token likelihood (Vaswani et al., 2017; Brown et al., 2020):

$$p(y_{1:L}, x_{1:L}) = p(y_{1:L} | x_{1:L}) p_\sigma(x_{1:L}). \quad (26)$$

Here  $p(y | x)$  is exactly what is used in practice: given embeddings (hidden states), the decoder head produces categorical distributions over tokens at each position. The prior  $p_\sigma(x)$  is the new object made explicit by our latent-noise interpretation.

**MAP training objective.** In the full token model we view the categorical decoder as a likelihood and the embedding prior as a prior. Given a token sequence  $y_{1:L}$ , we estimate parameters by *maximum a posteriori* (MAP):

$$(\hat{\theta}, \hat{\phi}) \in \arg \max_{\theta, \phi} \log P_\theta(y_{1:L} | x_{1:L}) + \log p_{\phi, \sigma}(x_{1:L}), \quad (27)$$

equivalently minimizing the negative log-posterior, which is precisely cross-entropy plus the prior-induced stability term (up to constants and weighting). In the next section we (i) specify  $p(y | x)$  in the standard way, (ii) show how marginalizing the embeddings yields

a well-defined sequence likelihood  $p(y)$ , and (iii) explain why it is important (for learning across multiple sequences) that  $p(y)$  defines a consistent stochastic process (Kolmogorov-style) (Billingsley, 1995). This will let us write down and optimize the augmented log-likelihood over pairs  $\{(y^{(i)}, x^{(i)})\}$ , in which the margin/barrier term enters as a principled, model-implied regularizer. The key insight is that LLMs can be fit using the same training machinery; the only modification is the addition of the log-prior term, which is straightforward to incorporate and leads to more robust model fitting.

Section 5 introduces the full model  $p(y | x) p_\sigma(x)$  and its marginal  $p(y)$ , and establishes consistency across sequence lengths (Kolmogorov-style), so the model assigns coherent probabilities to variable-length token sequences and datasets (Billingsley, 1995).

## 5 A Token-Level Stochastic Process Induced by the Embedding Prior

So far we have constructed an explicit embedding prior  $p_\sigma(x_{1:n})$  induced by causal self-attention. To connect this to real transformer language modeling, we now combine this prior with the usual categorical decoder likelihood  $P(y | x)$  (Vaswani et al., 2017; Brown et al., 2020) and study the induced token law  $\{P(y_{1:n})\}_{n \geq 1}$ . Our main result is that, under strict causality, these finite-dimensional token distributions are consistent across sequence length and therefore define a bona fide stochastic process over infinite token sequences via standard extension theorems (Billingsley, 1995; Kolmogorov, 1950). This gives a rigorous probabilistic foundation for viewing a causal transformer as a single law over variable-length token sequences. Readers primarily interested in the practical modeling consequences may skip the proofs and proceed; all measure-theoretic proofs are deferred to Appendix C.

### 5.1 From the embedding prior to a token-level law

Let  $V = \{v_1, \dots, v_K\}$  be a finite vocabulary, equipped with the discrete  $\sigma$ -algebra  $2^V$ . For each  $n \geq 1$ , the length- $n$  token space is  $V^n$ , and the infinite token space is the product  $V^\infty = \prod_{t=1}^\infty V$ , endowed with the product  $\sigma$ -algebra generated by cylinder sets (Billingsley, 1995).

Given latent embeddings  $x_{1:n}$ , we use the standard transformer decoder likelihood

$$P(y_{1:n} | x_{1:n}) = \prod_{t=1}^n P(y_t | y_{<t}, x_{1:n}), \quad (28)$$

where each factor is a categorical distribution over  $V$  (typically a softmax computed from the final hidden state at position  $t$ ). This is exactly the observation model used in practice.

We pair this with the causal attention embedding prior developed earlier:

$$x_t = \mu_t(x) + \varepsilon_t, \quad \varepsilon_t \sim \mathcal{N}(0, \sigma^2 I_d), \quad (29)$$

with strict causal masking in  $\mu_t$  (only  $s < t$  contribute), and with the Jacobian non-degeneracy assumptions from Section 3 so that  $p_\sigma(x_{1:n})$  is well-defined.

Together, these define the joint model

$$P(y_{1:n}, x_{1:n}) = P(y_{1:n} | x_{1:n}) p_\sigma(x_{1:n}), \quad (30)$$

and hence the marginal token likelihood

$$P(y_{1:n}) = \int_{\mathbb{R}^{dn}} P(y_{1:n} | x_{1:n}) p_{\sigma}(x_{1:n}) dx_{1:n}. \quad (31)$$

Equation (31) is the key object in this section: it is the token-level law induced by the probabilistic transformer, obtained by integrating out latent embeddings.

## 5.2 Consistency across sequence lengths

To learn from datasets containing sequences of different lengths, and to interpret the model as a single probabilistic object rather than a separate model for each  $n$ , the family  $\{P(y_{1:n})\}_{n \geq 1}$  must be *projectively consistent* (Billingsley, 1995). In the present setting, strict causality is exactly what makes this possible.

**Theorem 2** (Kolmogorov consistency). *Assume strict causal masking and Jacobian non-degeneracy so that  $p_{\sigma}(x_{1:n})$  exists for each  $n$ . Then for all  $n \geq 2$  and all  $y_{1:n-1} \in V^{n-1}$ ,*

$$\sum_{y_n \in V} P(y_{1:n}) = P(y_{1:n-1}), \quad (32)$$

where the right-hand side is the marginal likelihood obtained from the  $(n - 1)$ -dimensional model.

The role of causality is essential: without it, consistency can fail.

**Proposition 2** (Non-causal attention breaks consistency). *If attention is non-causal (future positions may influence the attention normalization at earlier positions), then in general the family  $\{P(y_{1:n})\}_{n \geq 1}$  induced by (31) is not projectively consistent, and (32) need not hold.*

Taken together, Theorem 2 and Proposition 2 show that strict causality is not merely a computational convenience here; it is the structural property that makes the induced family of token laws mathematically coherent across sequence lengths.

## 5.3 Infinite-sequence law and dataset-level likelihood

Once projective consistency holds, standard extension theory yields a unique probability measure on the infinite product space.

**Theorem 3** (Transformer stochastic process). *Under the assumptions of Theorem 2, there exists a unique probability measure  $P$  on  $(V^{\infty}, \mathcal{F})$  such that for every  $n \geq 1$  and every  $y_{1:n} \in V^n$ ,*

$$P(Y_1 = y_1, \dots, Y_n = y_n) = P(y_{1:n}), \quad (33)$$

where  $(Y_t)_{t \geq 1}$  are the coordinate projections on  $V^{\infty}$ .

This immediately gives a principled interpretation of learning on datasets. If  $\{y^{(i)}\}_{i=1}^N$  is a collection of variable-length sequences, then (up to truncation) these may be viewed as draws from the same underlying process. One may therefore optimize the marginal objective

$$\sum_{i=1}^N \log P(y_{1:n_i}^{(i)}),$$

or, if one wishes to retain latent embeddings explicitly, optimize the augmented objective

$$\sum_{i=1}^N \log P(y_{1:n_i}^{(i)}, x_{1:n_i}^{(i)}) = \sum_{i=1}^N \log P(y_{1:n_i}^{(i)} | x_{1:n_i}^{(i)}) + \sum_{i=1}^N \log p_\sigma(x_{1:n_i}^{(i)}), \quad (34)$$

where the embedding prior term contributes the model-implied stability / margin regularization. This is the probabilistic basis for MAP-style estimation in the transformer setting developed in the previous sections.

## 6 Depth: $L$ -Layer Composition as Hierarchical Conditional Priors

The previous sections analyzed a *single* causal attention map as a latent-noise generator of embeddings and showed that token-dependent attention induces an additional stability term in the exact likelihood via change-of-variables (Papamakarios et al., 2021). We now explain how this probabilistic view composes across depth. This section may be skipped on a first reading without loss of continuity.

The key message is structural: a deep causal transformer naturally defines a *hierarchy* of conditional priors over layerwise embeddings. Moreover, under the standard architectural convention — that attention weights in layer  $\ell$  are computed from the previous-layer embeddings  $x^{(\ell-1)}$  as in standard transformer blocks (Vaswani et al., 2017; Ba et al., 2016) — the nontrivial stability correction induced by token-dependent mixing *localizes* to the first such token-dependent map. This makes it possible to capture the main geometric effect with an embedding-level “attention prior” module, while leaving the rest of a deep network unchanged.

### 6.1 Setup: layer-wise embeddings and latent noise

Let  $L_{\text{layers}}$  denote the number of transformer layers, and let

$$x_{1:T}^{(0)} \in (\mathbb{R}^d)^T$$

be the input token embeddings (including positional encodings). For each layer  $\ell \in \{1, \dots, L_{\text{layers}}\}$ , we introduce latent noise

$$\varepsilon_{1:T}^{(\ell)} = (\varepsilon_1^{(\ell)}, \dots, \varepsilon_T^{(\ell)}), \quad \varepsilon_t^{(\ell)} \in \mathbb{R}^d, \quad \varepsilon_t^{(\ell)} \sim \mathcal{N}(0, \sigma_\ell^2 I_d),$$

and we view the layer output embeddings  $x_{1:T}^{(\ell)}$  as generated by a causal layer map plus noise. To keep the exposition focused on attention, we write a generic layer transformation as

$$x_t^{(\ell)} = g_t^{(\ell)}(x_{1:t}^{(\ell-1)}) + \varepsilon_t^{(\ell)}, \quad t = 1, \dots, T, \quad (35)$$

where causality means  $g_t^{(\ell)}$  depends only on the prefix  $x_{1:t}^{(\ell-1)}$  (via masking). In a standard transformer block,  $g^{(\ell)}$  comprises (multi-head) causal self-attention applied to  $x^{(\ell-1)}$ , followed by MLP and residual/normalization structure (Vaswani et al., 2017; Ba et al., 2016); our results below only use the fact that  $g^{(\ell)}$  is *computed from*  $x^{(\ell-1)}$  and does not depend on the current-layer noise  $\varepsilon^{(\ell)}$ .

Equation (35) induces a residual map for each layer,

$$\varepsilon_t^{(\ell)} = e_t^{(\ell)}(x^{(\ell)}, x^{(\ell-1)}) \triangleq x_t^{(\ell)} - g_t^{(\ell)}(x_{1:t}^{(\ell-1)}). \quad (36)$$

This map is *explicit* (forward-generative) as written: once  $x^{(\ell-1)}$  is fixed,  $x^{(\ell)}$  is an additive-noise perturbation around  $g^{(\ell)}(x^{(\ell-1)})$ .

## 6.2 Hierarchical conditional-prior factorization

Because (35) is causal in  $t$ , it defines a layer-wise conditional prior that factors over positions:

$$p_{\sigma_\ell} \left( x_{1:T}^{(\ell)} \mid x_{1:T}^{(\ell-1)} \right) = \prod_{t=1}^T \mathcal{N} \left( x_t^{(\ell)} ; g_t^{(\ell)} (x_{1:t}^{(\ell-1)}), \sigma_\ell^2 I_d \right). \quad (37)$$

Stacking layers yields a *hierarchical* latent-variable model over embeddings:

$$p \left( x_{1:T}^{(1)}, \dots, x_{1:T}^{(L_{\text{layers}})} \mid x_{1:T}^{(0)} \right) = \prod_{\ell=1}^{L_{\text{layers}}} p_{\sigma_\ell} \left( x_{1:T}^{(\ell)} \mid x_{1:T}^{(\ell-1)} \right). \quad (38)$$

Equation (38) is the formal sense in which depth composes as a hierarchy of conditional priors: each layer defines a stochastic transition on embeddings, driven by latent noise, and the deep model is their composition.

## 6.3 Exact likelihood and triangular structure across depth

As in the single-layer analysis, one can compute the exact embedding density induced by the latent noises via change-of-variables (Papamakarios et al., 2021). Here it is convenient to work with the full collection of latent variables

$$\varepsilon \triangleq \{ \varepsilon_{1:T}^{(\ell)} \}_{\ell=1}^{L_{\text{layers}}} \quad \text{and} \quad x \triangleq \{ x_{1:T}^{(\ell)} \}_{\ell=1}^{L_{\text{layers}}}.$$

Define the global residual map  $E$  by stacking (36) over all  $(\ell, t)$ :

$$\varepsilon = E(x; x^{(0)}).$$

With causal masking, the Jacobian of  $E$  with respect to  $x$  is block lower-triangular under a natural ordering of variables (e.g., increasing  $(\ell, t)$ ). Therefore,

$$\log p(x \mid x^{(0)}) = \log p(\varepsilon) + \log |\det J_{x \rightarrow \varepsilon}(x)| = \sum_{\ell, t} \log p(\varepsilon_t^{(\ell)}) + \sum_{\ell, t} \log \left| \det \left( \frac{\partial e_t^{(\ell)}}{\partial x_t^{(\ell)}} \right) \right|. \quad (39)$$

The proofs of triangularity and the determinant decomposition are standard and are deferred to Appendix D.

## 6.4 Localization of the stability correction under standard conditioning

The single-layer results showed that the stability/log-determinant term becomes nontrivial when the context summary depends on the *current* embedding being generated (token-dependent mixing in the same variable). In the multi-layer setting (35), the standard transformer convention is that the attention weights in layer  $\ell$  are computed from  $x^{(\ell-1)}$ , not from  $x^{(\ell)}$ . Under this convention, the layer-wise residual map (36) is affine in  $x_t^{(\ell)}$ , which implies the diagonal derivative is the identity.

**Proposition 3** (No layer-wise stability correction under previous-layer conditioning). *Assume that for each layer  $\ell \geq 2$ , the layer map  $g_t^{(\ell)}$  depends only on  $x_{1:t}^{(\ell-1)}$  and does not depend on  $x^{(\ell)}$ . Then for every  $t$ ,*

$$\frac{\partial e_t^{(\ell)}}{\partial x_t^{(\ell)}} = I_d, \quad \text{hence} \quad \log \left| \det \left( \frac{\partial e_t^{(\ell)}}{\partial x_t^{(\ell)}} \right) \right| = 0. \quad (40)$$

Proposition 3 says: once the attention pattern used to generate a layer is computed from the previous layer, that layer contributes *only* the Gaussian energy term  $\|x_t^{(\ell)} - g_t^{(\ell)}(x_{1:t}^{(\ell-1)})\|_2^2$  and no additional stability factor.

Where, then, does the nontrivial stability term live in a deep model? It lives precisely in whichever stage uses token-dependent mixing *with respect to the variable being generated*. In this paper, that stage is the embedding-level attention prior analyzed earlier: a causal attention map that mixes past *values* using weights that depend on the current *query* formed from the same embedding variable, producing the diagonal block  $I_d - \Sigma_t A$  and the margin/barrier term.

**Corollary 6.1** (Localization to a single attention-prior stage). *Consider a deep model in which: (i) the first stage defines an embedding-level attention prior of the form analyzed in Section 3, and (ii) all subsequent layers satisfy the previous-layer conditioning assumption of Proposition 3. Then the total stability/log-determinant contribution in (39) is exactly the single-layer stability term from the attention-prior stage; deeper layers contribute zero.*

Corollary 6.1 formalizes the practical takeaway used later in our experiments: the margin/barrier term implied by token-dependent causal mixing can be captured by a single lightweight module acting on embeddings, without altering the rest of a deep transformer stack.

The “no correction” result is not a claim that depth is irrelevant; it is a statement about where the exact change-of-variables stability factor appears. If a layer is modified so that its attention weights depend on the current-layer variable being generated (e.g., by defining an implicit self-consistency equation at that layer, or by using token-dependent mixing in the residualization variable), then the diagonal derivative  $\partial e_t^{(\ell)} / \partial x_t^{(\ell)}$  is no longer the identity and an additional stability term appears — with an analogous “margin to degeneracy” interpretation. We do not pursue these variants here, but the analysis in Section 3 can be applied layer-wise.

## 6.5 Multi-head attention, residual pathways, and normalization

The statements in Section 6 were written for a generic causal layer map  $g_t^{(\ell)}(\cdot)$  to keep notation light. We now briefly connect this abstraction to a standard transformer block with multi-head attention, MLP, residual connections, and normalization.

A typical pre-norm transformer block (one layer) can be written schematically as

$$u_{1:T}^{(\ell)} = x_{1:T}^{(\ell-1)} + \text{MHA}^{(\ell)}\left(\text{LN}\left(x_{1:T}^{(\ell-1)}\right)\right), \quad (41)$$

$$\tilde{x}_{1:T}^{(\ell)} = u_{1:T}^{(\ell)} + \text{MLP}^{(\ell)}\left(\text{LN}\left(u_{1:T}^{(\ell)}\right)\right), \quad (42)$$

where  $\text{MHA}^{(\ell)}$  denotes masked (causal) multi-head self-attention and LN is layer normalization. In our latent-noise view, we can introduce stochasticity at the layer output via

$$x_t^{(\ell)} = \tilde{x}_t^{(\ell)} + \varepsilon_t^{(\ell)}, \quad \varepsilon_t^{(\ell)} \sim \mathcal{N}(0, \sigma_\ell^2 I_d). \quad (43)$$

Equivalently, (41) to (43) defines the layer map  $g_t^{(\ell)}(x_{1:t}^{(\ell-1)}) \triangleq \tilde{x}_t^{(\ell)}$  appearing in (35).

**Remark** Proposition 3 (no additional stability/log-determinant correction from deeper layers) continues to hold for standard transformer blocks with multi-head attention, residual pathways, MLPs, and normalization, provided the following *conditioning convention* is respected:

For each layer  $\ell$ , the attention weights used inside  $\text{MHA}^{(\ell)}$  are computed from the previous-layer embeddings (e.g., from  $\text{LN}(x^{(\ell-1)})$ ), and the layer noise  $\varepsilon^{(\ell)}$  enters additively at the output as in (43).

Under this convention, the residual map at layer  $\ell$  has the form  $e_t^{(\ell)} = x_t^{(\ell)} - g_t^{(\ell)}(x_{1:t}^{(\ell-1)})$  and is *affine* in  $x_t^{(\ell)}$ , so  $\partial e_t^{(\ell)} / \partial x_t^{(\ell)} = I_d$  and the layer contributes no extra stability factor in (39). The geometric “margin/log-barrier” effect therefore appears only in stages where the attention pattern depends on the *current* embedding variable being generated (as in our embedding-level attention prior), not in layers whose attention patterns are computed from earlier representations.

If a layer is modified so that its attention weights depend on  $x^{(\ell)}$  itself (for example via an implicit/self-consistent layer definition, or by placing  $x^{(\ell)}$  inside the queries used in the softmax for the same layer variable), then  $\partial e_t^{(\ell)} / \partial x_t^{(\ell)}$  is no longer the identity and that layer will contribute its own stability/log-determinant term with an analogous margin-to-degeneracy interpretation.

## 7 Experiments

In this section, we empirically validate our theoretical results using a controlled dataset. While large-scale model training in industrial settings is beyond the scope of this paper, we hope these initial results encourage further investigation and lead to practical insights for robust foundation models.

### 7.1 Shared experimental setup

We use WikiText-2 (Merity et al., 2017) at the character level. The training set has approximately 10.9M characters. We retain the 114 characters that appear at least 50 times in the training set and map all remaining (unknown) characters to a single `<unk>` token, giving a vocabulary of  $|\mathcal{V}|=115$ . The validation split ( $\sim 1.15\text{M}$  characters) is used for all reported metrics; the test split is held out. Character-level tokenization avoids external tokenizer dependencies and keeps the vocabulary small enough for the model to train from scratch in a controlled setting.

We train a small causal GPT (SmallGPT):  $d=128$ , 4 attention heads, 2 transformer blocks, context length  $T=512$ . This architecture has  $\sim 396\text{K}$  transformer parameters plus  $\sim 95\text{K}$  embedding parameters. It matches the hierarchical view in Section 6: we pair a deep observation model (the 2-layer GPT) with a single embedding-level attention-prior stage, and use the standard-conditioning localization results (Proposition 3, Corollary 6.1) to justify focusing the nontrivial stability correction at the embedding level.

The `EmbeddingPrior` is a single causal attention layer parameterized by a learnable  $d \times d$  matrix  $W$  that computes the attention-weighted covariance  $\Sigma_t$  and the log-Jacobian margin term  $-\sum_t \log |\det(\text{Id}_d - \Sigma_t W^\top)|$  (Theorem 1). We use the *margin-only* variant, since  $L_2$  regularization is unnecessary given the implicit regularization provided by SGD with small learning rates and early stopping. The MAP loss is  $\mathcal{L} = \mathcal{L}_{\text{CE}} + \lambda_m \cdot \mathcal{L}_{\text{margin}}$  with  $\lambda_m = 0.05$ , after dropping the quadratic residual term.

For proper comparison, both models (CE-only baseline and Margin-only) use identical architectures initialized with the same random seed. Optimizer: AdamW (lr= $10^{-3}$ , weight

decay  $10^{-4}$ ); cosine learning-rate schedule; 30 epochs; batch size 64; gradient clipping at norm 1.0. All experiments run on a single H100 GPU.

We report bits-per-character (BPC) =  $\mathcal{L}_{\text{CE}}/\ln 2$  as the primary predictive-quality metric.

## 7.2 WikiText-2 training: CE-only vs. Margin-only (Figure 7.4)

We first demonstrate that the stability/margin term implied by the change-of-variables correction (Section 3) can be used as a drop-in auxiliary loss on real language data with only a modest change in predictive quality. This is an apples-to-apples comparison in the same training setup: same architecture, same optimizer, same seed; the only difference is whether the stability (log-barrier) term is included in the objective (see Section 4 for the corresponding optimization view).

We train two SmallGPT models on WikiText-2 as described in Section 7.1. We report training and validation BPC at every epoch.

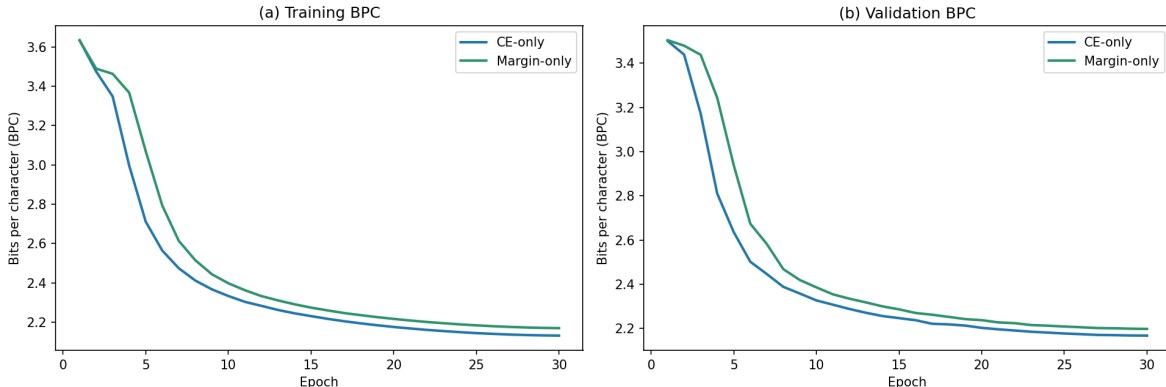


Figure 7.4: **WikiText-2 training curves.** Bits-per-character (BPC) on WikiText-2 over 30 epochs for CE-only (blue) and Margin-only (green,  $\lambda_m=0.05$ ). (a) Training BPC: both modes converge along nearly identical trajectories, with the margin-regularized model tracking the baseline closely throughout. (b) Validation BPC: the final gap is 0.030 BPC (CE-only: 2.168, Margin-only: 2.198), a relative difference of 1.4%. The margin regularizer preserves predictive quality while imposing the theory-derived dispersion penalty as an additional training signal.

Both models converge smoothly with nearly overlapping curves (Figure 7.4). The final validation BPC values are:

Mode	Train BPC	Val BPC
CE-only	2.132	2.168
Margin-only	2.170	2.198

The 0.030 BPC gap (1.4% relative) confirms that the margin term acts as a mild regularizer rather than a competing objective: it does not distort the CE landscape. This is the expected behavior for a MAP objective: the prior contributes a regularization pressure that shapes the geometry of learned representations without substantially altering the observation-model fit. For a 2-layer character-level model trained for 30 epochs, a final BPC in the 2.1–2.2 range is consistent with prior work on small-scale character-level language models.

### 7.3 Robustness to embedding noise (Figure 7.5)

Next, we test whether the stability/margin term improves robustness to perturbations in embedding space. The theory shows that the exact embedding log prior includes a log-volume (stability) factor that becomes large in magnitude near degeneracy (Section 3), and the optimization view interprets this as a margin/log-barrier that discourages locally ill-conditioned configurations (Section 4). We therefore expect models trained with the stability term to degrade more gracefully when embeddings are corrupted.

After training, we evaluate both models on the validation set with additive Gaussian noise  $\mathcal{N}(0, \sigma^2 I)$  injected into the embedding layer. We sweep  $\sigma \in [0, 0.5]$  with 11 equally spaced values, averaging each noise level over 5 independent draws for stability, and we report absolute BPC and relative degradation (BPC at noise  $\sigma$  divided by clean BPC).

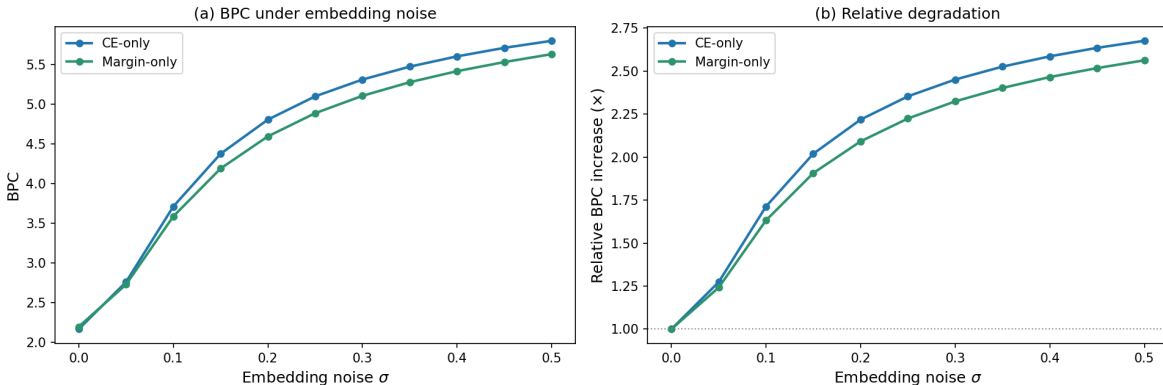


Figure 7.5: **BPC under embedding noise on WikiText-2.** (a) Absolute BPC as a function of Gaussian noise standard deviation  $\sigma$  added to embeddings. Margin-only (green) remains consistently below CE-only (blue) across the entire noise range, with the gap widening at higher noise levels. (b) Relative degradation (noisy BPC / clean BPC): CE-only degrades to  $2.68\times$  its clean performance at  $\sigma=0.5$ , while Margin-only degrades only  $2.56\times$ —a 12 percentage-point improvement in robustness. The margin regularizer provides measurable protection against embedding perturbations, consistent with the stability-margin interpretation.

Mode	Clean BPC	BPC at $\sigma=0.5$	Degradation ( $\times$ )
CE-only	2.168	5.802	2.68
Margin-only	2.198	5.634	2.56

The robustness advantage of Margin-only is visible across the full noise range (Figure 7.5). At every noise level  $\sigma > 0$ , the margin-regularized model achieves lower absolute BPC than the baseline, despite starting from a slightly higher clean BPC (2.198 vs. 2.168).

The relative-degradation panel (Figure 7.5b) isolates the structural effect: even after normalizing for the baseline-performance difference, the margin-regularized model degrades more gracefully. The gap in relative degradation grows monotonically with  $\sigma$ , reaching 12 percentage points at  $\sigma=0.5$ . This is consistent with the margin interpretation: the regularizer encourages the model to maintain a safety buffer from the Jacobian degeneracy boundary, and this buffer translates into resilience when embeddings are perturbed.

Notably, the crossover in absolute BPC occurs between  $\sigma=0.0$  and  $\sigma=0.05$ : the margin-only model pays a small premium in clean BPC but overtakes the baseline as soon as any noise is present. This is exactly the trade-off predicted by the MAP formulation: the prior term slightly penalizes maximum-likelihood fit in exchange for a more robust representation geometry.

#### 7.4 Regularization path: the effect of $\lambda_m$ (Figure 7.6)

Finally, we characterize the full trade-off landscape as the margin penalty weight  $\lambda_m$  varies, analogous to a Lasso regularization path.

The theory (Section 4) predicts that increasing  $\lambda_m$  should (i) increase the stability margin (moving away from degeneracy) and (ii) improve robustness to embedding perturbations, while potentially degrading clean predictive quality if the penalty is too strong. Understanding this trade-off is critical for practitioners: it determines how to select  $\lambda_m$  via cross-validation, much as one selects the  $\ell_1$  penalty in Lasso regression.

We train seven independent models with  $\lambda_m \in \{0, 0.005, 0.01, 0.02, 0.05, 0.1, 0.2\}$ , all sharing the same architecture, optimizer, and random seed (Section 7.1). For each trained model, we measure three diagnostics on the validation set:

1. **Validation BPC** (clean and under noise  $\sigma=0.3$ ): predictive quality and robustness.
2. **Normalized  $\text{Var}_a$** :  $\text{tr}(\Sigma_t)/\text{RMS}(x)^2$ , which removes the embedding-scale confound and isolates the structural dispersion effect.
3. **Signal-to-noise ratio (SNR)**:  $\|x\|_{\text{RMS}}/\|e\|_{\text{RMS}}$  where  $e_t = x_t - \mu_t$  is the prior’s residual. Higher SNR means the prior explains a larger fraction of the embedding variance.

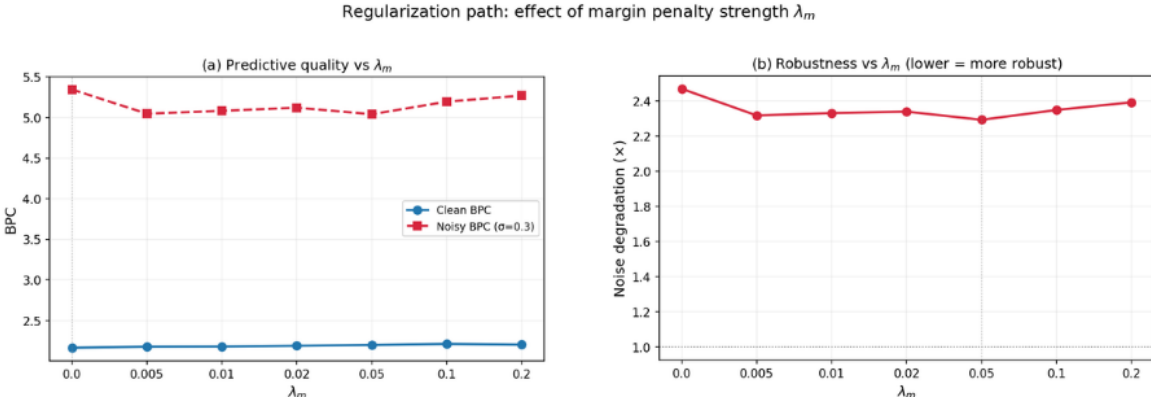


Figure 7.6: **Regularization path as a function of  $\lambda_m$ .** Seven models trained with margin penalty weights  $\lambda_m \in \{0, 0.005, 0.01, 0.02, 0.05, 0.1, 0.2\}$ . (a) Validation BPC: clean (blue) rises only 2% across the full  $\lambda_m$  range, while noisy BPC (red,  $\sigma=0.3$ ) exhibits a U-shape with minimum at  $\lambda_m=0.05$  (5.040 vs. 5.345 baseline — a 6% improvement). (b) Noise degradation ratio: U-shaped with optimum at  $\lambda_m=0.05$  (2.29 $\times$  vs. 2.47 $\times$  baseline), a 7% improvement in robustness.

The regularization path (Figure 7.6, Table 1) reveals a clear and instructive trade-off with a well-defined optimum across the reported metrics:

Table 1: Lambda sweep results on WikiText-2.  $\text{BPC}_\sigma$  denotes validation BPC under Gaussian noise  $\sigma=0.3$ .  $\text{Deg} = \text{BPC}_\sigma / \text{BPC}$ .  $\text{SNR} = \|x\|/\|e\|$ .  $\text{Var}_{a,n} = \text{tr}(\Sigma_t)/\text{RMS}(x)^2$ . The optimal robustness (lowest degradation ratio) occurs at  $\lambda_m=0.05$  (**bold**). At  $\lambda_m=0$  no prior is trained, so SNR and  $\text{Var}_{a,n}$  are not applicable.

$\lambda_m$	BPC	$\text{BPC}_\sigma$	Deg ( $\times$ )	SNR	$\text{Var}_{a,n}$
0.000	2.165	5.345	2.47	—	—
0.005	2.179	5.047	2.32	0.900	122.81
0.010	2.181	5.082	2.33	0.893	128.38
0.020	2.190	5.121	2.34	0.876	124.77
<b>0.050</b>	<b>2.199</b>	<b>5.040</b>	<b>2.29</b>	<b>0.878</b>	<b>122.22</b>
0.100	2.213	5.195	2.35	0.899	126.49
0.200	2.203	5.269	2.39	0.895	126.70

**(a) Predictive quality: a remarkably flat clean-BPC curve.** Clean validation BPC rises only from 2.165 to 2.213 across two orders of magnitude of  $\lambda_m$  — a total range of just 2.2%. This is the first key result: *the margin penalty barely affects clean predictive quality*. The observation model (GPT) retains its expressive power because the prior operates solely on embeddings, orthogonal to the transformer’s internal computation.

Under noise ( $\sigma=0.3$ ), the picture changes dramatically. Noisy BPC drops from 5.345 (baseline) to a **minimum of 5.040 at  $\lambda_m=0.05$**  — a **5.7% improvement**. At the optimal point, the model pays only 1.6% in clean BPC (2.199 vs. 2.165) while gaining 5.7% in noisy-condition performance. This is a highly favorable trade-off.

Beyond  $\lambda_m=0.05$ , noisy BPC rises again: the penalty becomes strong enough to over-constrain the representation geometry, reducing the model’s ability to recover from perturbations. The resulting U-shape is the hallmark of a well-behaved regularizer with a tunable optimum.

**(b) Dispersion and SNR.** The normalized  $\text{Var}_a$  remains relatively stable across all nonzero  $\lambda_m$  values, ranging from approximately 122 to 128. This suggests that the structural dispersion captured by the trained prior is robust to the regularization strength. The SNR dips from 0.900 at  $\lambda_m=0.005$  to 0.876 at  $\lambda_m=0.02$ , then partially recovers at higher  $\lambda_m$ , indicating that at moderate regularization the prior captures more context-dependent variation relative to the overall embedding scale.

**(c) Robustness: optimum at  $\lambda_m=0.05$ .** The noise degradation ratio (noisy BPC / clean BPC) drops from  $2.47\times$  at  $\lambda_m=0$  to a **minimum of  $2.29\times$  at  $\lambda_m=0.05$**  — a **7.3% improvement in robustness**. Beyond this optimum, the ratio rises to  $2.35\text{--}2.39\times$  at  $\lambda_m=0.1\text{--}0.2$ , reflecting the onset of over-regularization.

The U-shape confirms the stability-margin interpretation: moderate  $\lambda_m$  pushes  $\det(\text{Id}_d - \Sigma_t A)$  away from zero (larger margin), yielding more graceful degradation under perturbation. Too-large  $\lambda_m$  overconstrains the embedding geometry, reducing the model’s representational capacity and partially undoing the robustness benefit.

**Connection to the SVM/margin analogy.** The regularization path provides direct empirical support for the large-margin interpretation developed in Section 4. In an SVM, the regularization parameter  $C$  trades off margin width against training error; the optimal  $C$

is found by cross-validation. Here,  $\lambda_m$  plays exactly this role: it controls how strongly the model is pushed away from the Jacobian degeneracy boundary  $\det(\text{Id}_d - \Sigma_t A) = 0$ . The optimal  $\lambda_m^* \approx 0.05$  is the point where the margin is wide enough to confer robustness without sacrificing too much predictive quality — the analogue of the optimal soft-margin SVM. The U-shaped degradation curve confirms that the margin penalty behaves as a well-tuned regularizer across a broad range of penalty strengths, with a clear optimum balancing predictive quality against robustness to perturbation.

## 7.5 Summary

Overall, these results confirm that the theoretical margin constraints translate smoothly into practical model training. The dispersion penalty preserves clean predictive quality while inducing a highly structured, coherent representation space that is significantly more resilient to noise.

## 8 Related Work

Our contribution connects three broad lines of research: (i) mechanisms and interpretations of self-attention in transformers, (ii) probabilistic modeling via latent variables and change-of-variables objectives, and (iii) stability, margins, and regularization viewpoints in modern ML. We highlight the closest connections and clarify what is distinct about the present framework.

Transformers introduced self-attention as a computational primitive for sequence transduction and autoregressive generation (Vaswani et al., 2017). A large empirical and theoretical literature studies what attention computes and how it shapes context use, including work on locality, sparsity, and inductive biases of attention patterns. Our focus is complementary: rather than proposing a new attention mechanism, we ask what *probabilistic object* is induced when causal attention is treated as a token-dependent generative rule over continuous hidden-state embeddings. This viewpoint makes explicit an additional, model-implied term in the embedding likelihood that can be interpreted as a stability/margin effect, and it provides an optimization lens that is directly actionable in training.

Normalizing flows formalize exact-likelihood density modeling by composing invertible maps and accounting for local volume change via the change-of-variables formula (Papamakarios et al., 2021). A central design principle is to choose transformations with tractable Jacobian determinants, e.g., coupling layers (Dinh et al., 2017) and autoregressive constructions such as IAF/MAF (Kingma et al., 2016; Papamakarios et al., 2017). Unlike the flow literature, we do not design a new invertible architecture. Instead, we observe that *standard causal self-attention*, viewed as a latent-noise transformation on embeddings, already induces an exact embedding likelihood with a nontrivial local-volume term. Our main technical results compute this term for causal attention and interpret it geometrically through a margin-to-degeneracy / log-barrier perspective.

A classical lesson from latent-variable modeling is that deterministic estimators often arise as limits of probabilistic models. A canonical example is probabilistic PCA, where standard PCA is recovered in a limiting (small-noise) regime (Tipping and Bishop, 1999). Our treatment of embeddings as latent variables plays a similar conceptual role: the noise scale provides an optimization lens that connects an explicit probabilistic embedding prior to familiar deterministic behavior, while the stability term remains as a principled geometric correction in the exact likelihood.

Large-margin classifiers provide a geometric view of learning in which a small set of constraints (support vectors) governs robustness and generalization (Cortes and Vapnik, 1995). Separately, interior-point methods use log-barriers as smooth relaxations of hard constraints, offering a principled way to trade off objective fit against constraint satisfaction. Our contribution is not to import these tools directly, but to show that an analogous barrier-like mechanism emerges *from the exact likelihood* induced by token-dependent causal attention: the additional term behaves as a stability factor and naturally defines a margin to a critical degeneracy boundary. This yields a practical training lever that can be tuned analogously to a regularization path.

To connect embedding priors to token modeling at the dataset level, it is important that the resulting family of finite-dimensional token distributions is consistent across sequence lengths. This is the classical setting of projective consistency and extension to a stochastic process (Kolmogorov-style) (Billingsley, 1995; Kolmogorov, 1950). In our setting, causality (masking) is the key structural ingredient that enables such consistency, while non-causal attention can break it. We treat this as a technical foundation for learning from variable-length sequences under an explicit probabilistic model.

In summary, our approach distinguishes itself from existing work on attention mechanisms and from flow- and margin-based literature by (i) treating hidden-state embeddings as latent variables governed by a causal attention prior, (ii) computing the exact local-volume correction induced by token-dependent attention, and (iii) interpreting the resulting likelihood term as a stability/margin/log-barrier effect that yields a lightweight, architecture-preserving training objective component.

## 9 Discussion and Future Directions

Our main contribution is conceptual and structural: by treating hidden-state embeddings as latent random variables and causal self-attention as a token-dependent latent-noise transformation, we obtain an *exact* embedding likelihood whose additional change-of-variables term induces a margin-to-degeneracy viewpoint. This re-frames causal self-attention as not only a context aggregator (Vaswani et al., 2017), but also a mechanism with an intrinsic stability geometry. The resulting barrier term is *model-implied* (not heuristic) and can be surfaced in training as a lightweight penalty without changing the transformer architecture.

The barrier is best understood as a conditioning constraint: it discourages trajectories that approach locally singular configurations of the attention-induced map. In this sense it is closer in spirit to classical stability constraints than to generic “make attention sparse” regularizers. The sign and strength of the effective coupling (e.g., the scalar  $a$  in the  $d=1$  analysis) determine how dispersion influences local sensitivity, but the degeneracy boundary and margin interpretation remain the invariant object: the likelihood assigns vanishing mass to configurations approaching singularity.

**Posterior-aware decoding beyond MAP.** The latent-noise formulation defines a posterior over embedding trajectories (and, in principle, intermediate layer states) conditioned on an observed prefix. This opens the door to decoding rules that go beyond a single point-estimate (MAP) embedding path. Conceptually, the next-token distribution can be written as an integral,

$$P(y_t | y_{<t}) = \int P(y_t | y_{<t}, x_{1:t}) p(x_{1:t} | y_{<t}) dx_{1:t},$$

and approximated by sampling or structured inference rather than collapsing  $x$  to one trajectory. Even coarse approximations that preserve the main geometry (staying away from near-degenerate configurations) may yield practical gains in calibration and controllability.

**Uncertainty as a first-class output.** Because the model assigns an explicit density to embedding trajectories, it becomes meaningful to report uncertainty measures tied directly to the latent representation. Natural candidates include posterior dispersion in embedding space, predictive variance under posterior samples, or proximity to degeneracy via the margin/log-barrier quantities derived in Sections 3–4. Such signals could be used to (i) flag low-confidence continuations, (ii) calibrate selective generation (abstain, ask a clarifying question, or trigger retrieval) in the spirit of selective prediction (Geifman and El-Yaniv, 2017), or (iii) adapt decoding hyper-parameters (temperature, top- $p$ ) in a principled, state-dependent manner rather than via fixed heuristics. This perspective is complementary to classical probability calibration work, which studies when predicted probabilities match empirical correctness (Guo et al., 2017).

**Sequential inference for long contexts.** The causal structure invites sequential inference algorithms that update uncertainty as the prefix grows. Promising directions include particle methods (SMC) (Doucet et al., 2001) and MCMC over latent embeddings conditioned on tokens. Hybrid particle-MCMC approaches (Andrieu et al., 2010) are also natural candidates when the posterior is highly structured and naive proposals mix poorly. In all cases, the barrier term can act as a principled prior factor that discourages proposals drifting into near-degenerate regions. Approximate filtering-style methods may also be useful if they preserve the key geometry while remaining computationally feasible at long context lengths.

**Robustness and hallucinations under distribution shift.** A practical hypothesis is that uncertainty-aware decoding informed by the latent posterior could reduce hallucinations. When the model enters regions of high posterior uncertainty or small margin (near-degenerate attention geometries), decoding could become more conservative (e.g., trigger retrieval/verification, lower entropy, ask for clarification, or refuse). Testing this requires evaluations explicitly designed around distribution shift, factuality, and selective generation, beyond perplexity-style metrics; surveys of hallucination phenomena and mitigation provide useful taxonomies and benchmarks for such evaluation (Huang et al., 2023).

**Scaling and implementation questions.** At scale, the key open questions are computational: how to enforce or approximate the log-barrier stably during training (e.g., low-rank or stochastic log-det estimators, spectral surrogates, clipping/barrier schedules, or constrained parameterizations), how to tune the tradeoff efficiently (warm-start regularization paths), and how to couple the penalty with modern optimizers and large-batch regimes. Establishing reliable large-scale wins will require careful ablations across model size, data regimes, and downstream tasks, and will clarify whether the strongest benefits come from training-time regularization, inference-time uncertainty-aware decoding, or alignment-style objectives built on uncertainty signals.

## References

- C. Andrieu, A. Doucet, and R. Holenstein. Particle markov chain monte carlo methods. *Journal of the Royal Statistical Society: Series B (Statistical Methodology)*, 72(3):269–342, 2010. doi: 10.1111/j.1467-9868.2009.00736.x.
- J. L. Ba, J. R. Kiros, and G. E. Hinton. Layer normalization. In *Advances in Neural Information Processing Systems (NeurIPS)*, 2016.
- P. Billingsley. *Probability and Measure*. Wiley, 3 edition, 1995.
- C. M. Bishop. *Pattern Recognition and Machine Learning*. Springer, 2006.
- S. Boyd and L. Vandenberghe. *Convex Optimization*. Cambridge University Press, 2004.
- T. B. Brown, B. Mann, N. Ryder, M. Subbiah, J. Kaplan, et al. Language models are few-shot learners. In *Advances in Neural Information Processing Systems (NeurIPS)*, 2020.
- C. Cortes and V. Vapnik. Support-vector networks. *Machine Learning*, 20(3):273–297, 1995.
- L. Dinh, J. Sohl-Dickstein, and S. Bengio. Density estimation using real NVP. In *International Conference on Learning Representations (ICLR)*, 2017.
- A. Dosovitskiy, L. Beyer, A. Kolesnikov, D. Weissenborn, X. Zhai, T. Unterthiner, M. Dehghani, et al. An image is worth 16x16 words: Transformers for image recognition at scale. In *International Conference on Learning Representations (ICLR)*, 2021.
- A. Doucet, N. de Freitas, and N. Gordon. *Sequential Monte Carlo Methods in Practice*. Springer, 2001.
- B. Efron, T. Hastie, I. Johnstone, and R. Tibshirani. Least angle regression. *The Annals of Statistics*, 32(2):407–499, 2004.
- Y. Geifman and R. El-Yaniv. Selective classification for deep neural networks. In *Advances in Neural Information Processing Systems (NeurIPS)*, 2017.
- C. Guo, G. Pleiss, Y. Sun, and K. Q. Weinberger. On calibration of modern neural networks. In *International Conference on Machine Learning (ICML)*, 2017.
- L. Huang, W. Yu, W. Ma, W. Zhong, Z. Feng, H. Wang, Q. Chen, W. Peng, X. Feng, B. Qin, and T. Liu. A survey on hallucination in large language models: Principles, taxonomy, challenges, and open questions. *arXiv preprint arXiv:2311.05232*, 2023.
- E. Ising. Beitrag zur theorie des ferromagnetismus. *Zeitschrift für Physik*, 31(1):253–258, 1925. doi: 10.1007/BF02980577.
- D. P. Kingma, T. Salimans, R. Jozefowicz, X. Chen, I. Sutskever, and M. Welling. Improved variational inference with inverse autoregressive flow. In *Advances in Neural Information Processing Systems*, 2016.
- A. N. Kolmogorov. *Foundations of the Theory of Probability*. Chelsea Publishing Company, 1950. English translation of the 1933 original.
- S. Merity, C. Xiong, J. Bradbury, and R. Socher. Pointer sentinel mixture models. In *Proceedings of the 5th International Conference on Learning Representations (ICLR)*, 2017.
- K. P. Murphy. *Machine Learning: A Probabilistic Perspective*. MIT Press, 2012.
- G. Papamakarios, T. Pavlakou, and I. Murray. Masked autoregressive flow for density estimation. In *Advances in Neural Information Processing Systems*, volume 30, 2017.
- G. Papamakarios, E. Nalisnick, D. J. Rezende, S. Mohamed, and B. Lakshminarayanan. Normalizing flows for probabilistic modeling and inference. *Journal of Machine Learning Research*, 22(57):1–64, 2021.
- A. Radford, J. Wu, R. Child, D. Luan, D. Amodei, and I. Sutskever. Language models are

unsupervised multitask learners. *OpenAI Technical Report*, 2019.

R. Tibshirani. Regression shrinkage and selection via the lasso. *Journal of the Royal Statistical Society: Series B (Statistical Methodology)*, 58(1):267–288, 1996.

M. E. Tipping and C. M. Bishop. Probabilistic principal component analysis. *Journal of the Royal Statistical Society: Series B (Statistical Methodology)*, 61(3):611–622, 1999.

A. Vaswani, N. Shazeer, N. Parmar, J. Uszkoreit, L. Jones, A. N. Gomez, L. Kaiser, and I. Polosukhin. Attention is all you need. *Advances in Neural Information Processing Systems*, 30, 2017.

## A Including the current token in the context ( $s \leq t$ )

The main text uses the *strictly causal* attention summary  $\mu_t = \sum_{s < t} \alpha_{ts} v_s$  to keep the autoregressive structure maximally transparent. Standard implementations of causal self-attention often include the current position as well (i.e., they allow  $s \leq t$ ). This appendix records the corresponding formulas and shows that the change-of-variables likelihood continues to acquire an additional log-determinant factor; the only difference is that the diagonal derivative includes an extra contribution from the explicit dependence of  $v_t$  on  $x_t$  and from the nonzero self-weight  $\alpha_{tt}$ .

**Setup.** Fix a single-head self-attention layer. Define

$$q_t = W_Q x_t, \quad k_s = W_K x_s, \quad v_s = W_V x_s,$$

and let the (masked) attention weights be

$$\alpha_{ts}(x) = \frac{\exp(q_t^\top k_s)}{\sum_{r \leq t} \exp(q_t^\top k_r)}, \quad s \leq t, \quad (44)$$

with context summary

$$\mu_t(x) = \sum_{s \leq t} \alpha_{ts}(x) v_s. \quad (45)$$

As in the main text, we define the latent-noise residual map

$$\varepsilon_t = e_t(x) \triangleq x_t - \mu_t(x), \quad \varepsilon_t \sim \mathcal{N}(0, \sigma^2 I_d). \quad (46)$$

**Useful identities.** Write  $\bar{v}_t \triangleq \sum_{s \leq t} \alpha_{ts} v_s = \mu_t(x)$  for the attention-weighted mean of the values, and define the attention-weighted covariance over values (now including  $s = t$ ):

$$\Sigma_t^{(\leq)} \triangleq \sum_{s \leq t} \alpha_{ts}(x) (v_s - \bar{v}_t)(v_s - \bar{v}_t)^\top \succeq 0. \quad (47)$$

For the softmax weights (44) with logits  $\ell_{ts} = q_t^\top k_s$ , the derivative w.r.t. the current query satisfies

$$\frac{\partial \alpha_{ts}}{\partial q_t} = \alpha_{ts} \left( k_s - \sum_{r \leq t} \alpha_{tr} k_r \right). \quad (48)$$

**Diagonal Jacobian block for  $s \leq t$ .** The diagonal block of the Jacobian of the residual map  $e_t(x) = x_t - \mu_t(x)$  equals

$$\frac{\partial e_t}{\partial x_t} = I_d - \frac{\partial \mu_t}{\partial x_t}.$$

We decompose  $\partial \mu_t / \partial x_t$  into two contributions:

(i) *Direct value-path term.* Since  $v_t = W_V x_t$  appears inside the sum with weight  $\alpha_{tt}$ ,

$$\left. \frac{\partial \mu_t}{\partial x_t} \right|_{\text{value path}} = \alpha_{tt} W_V. \quad (49)$$

(ii) *Weight-path term via the query.* The weights  $\alpha_{ts}$  depend on  $x_t$  through  $q_t = W_Q x_t$ . Using  $\frac{\partial \alpha_{ts}}{\partial x_t} = \left( \frac{\partial \alpha_{ts}}{\partial q_t} \right) W_Q$  and (48), one obtains

$$\begin{aligned} \left. \frac{\partial \mu_t}{\partial x_t} \right|_{\text{weight path}} &= \sum_{s \leq t} v_s \left( \frac{\partial \alpha_{ts}}{\partial x_t} \right) = \sum_{s \leq t} v_s \left( \frac{\partial \alpha_{ts}}{\partial q_t} \right) W_Q \\ &= \left( \sum_{s \leq t} \alpha_{ts} v_s k_s^\top - \bar{v}_t \left( \sum_{r \leq t} \alpha_{tr} k_r \right)^\top \right) W_Q \\ &= \left( \sum_{s \leq t} \alpha_{ts} (v_s - \bar{v}_t) k_s^\top \right) W_Q. \end{aligned} \quad (50)$$

In the common bilinear parameterization  $k_s = W_K x_s$  and  $v_s = W_V x_s$ , the bracketed term in (50) can be rewritten in terms of the covariance (47):

$$\sum_{s \leq t} \alpha_{ts} (v_s - \bar{v}_t) k_s^\top = \Sigma_t^{(\leq)} W_K^\top. \quad (51)$$

Substituting (49), (50), and (51) gives

$$\frac{\partial \mu_t}{\partial x_t} = \alpha_{tt} W_V + \Sigma_t^{(\leq)} W_K^\top W_Q. \quad (52)$$

Therefore the diagonal Jacobian block becomes

$$\boxed{\frac{\partial e_t}{\partial x_t} = I_d - \alpha_{tt} W_V - \Sigma_t^{(\leq)} A, \quad A \triangleq W_K^\top W_Q.} \quad (53)$$

**Specialization to  $W_V = I_d$ .** In the common simplified analysis where the values are taken as  $v_s = x_s$  (equivalently  $W_V = I_d$ ), (53) reduces to

$$\frac{\partial e_t}{\partial x_t} = (1 - \alpha_{tt}) I_d - \Sigma_t^{(\leq)} A. \quad (54)$$

This makes explicit the additional  $(1 - \alpha_{tt})$  contraction that appears solely because the current token is included in the context.

**Resulting log-determinant term.** As in the strict-causal case, the full Jacobian is block lower triangular in time under causality, hence

$$\det(J_{x \rightarrow \varepsilon}) = \prod_{t=1}^L \det\left(\frac{\partial e_t}{\partial x_t}\right). \quad (55)$$

Under the Gaussian base density, the induced log-density becomes

$$\log p(x_{1:L}) = -\frac{1}{2\sigma^2} \sum_{t=1}^L \|e_t(x)\|_2^2 + \sum_{t=1}^L \log \left| \det\left(I_d - \alpha_{tt} W_V - \Sigma_t^{(\leq)} A\right) \right| - Ld \log \sigma + \text{const}, \quad (56)$$

with  $e_t(x) = x_t - \mu_t(x)$  and  $\mu_t$  defined by (45). The second term is the analogue of the “missing term” in the strict-causal setting: it is again the exact change-of-variables correction induced by token-dependent attention.

**Relation to the strict-causal case.** If one excludes the current token ( $s < t$ ), then  $\alpha_{tt} = 0$  and the covariance excludes  $s = t$ , so (53) reduces to the main-text diagonal block

$$\frac{\partial e_t}{\partial x_t} = I_d - \Sigma_t^{(<)} A,$$

recovering the formulas in Section 3. In particular, including  $s = t$  does not remove the additional term in the likelihood; it only changes its exact form by adding the explicit self-value contribution  $\alpha_{tt} W_V$  and replacing  $\Sigma_t^{(<)}$  by  $\Sigma_t^{(\leq)}$ .

## B Proofs for Section 3

Throughout, we work in the *strict-causal* setting  $s < t$  as in (2)–(4), with

$$\mu_t(x) = \sum_{s < t} \alpha_{ts}(x) v_s, \quad e_t(x) = x_t - \mu_t(x),$$

and single-head bilinear logits

$$\ell_{ts} = q_t^\top k_s, \quad q_t = W_Q x_t, \quad k_s = W_K x_s.$$

We write  $\alpha_t$  for the vector  $(\alpha_{t1}, \dots, \alpha_{t,t-1})$  and use the standard softmax  $\alpha_{ts} = \exp(\ell_{ts}) / \sum_{r < t} \exp(\ell_{tr})$ .

### B.1 Two standard identities

**Lemma B.1** (Softmax Jacobian). *Let  $\alpha = \text{softmax}(\ell) \in \mathbb{R}^m$  with components  $\alpha_i = \exp(\ell_i) / \sum_{j=1}^m \exp(\ell_j)$ . Then*

$$\frac{\partial \alpha_i}{\partial \ell_j} = \alpha_i (\delta_{ij} - \alpha_j), \quad \text{i.e.,} \quad \frac{\partial \alpha}{\partial \ell} = \text{Diag}(\alpha) - \alpha \alpha^\top. \quad (57)$$

**Proof** Differentiate  $\alpha_i = \exp(\ell_i) / Z$  with  $Z = \sum_j \exp(\ell_j)$ . We have  $\partial \alpha_i / \partial \ell_j = \delta_{ij} \exp(\ell_i) / Z - \exp(\ell_i) \exp(\ell_j) / Z^2 = \alpha_i (\delta_{ij} - \alpha_j)$ .  $\square$

**Lemma B.2** (Attention-weighted covariance identity). Let  $\{v_s\}_{s<t} \subset \mathbb{R}^d$  with weights  $\alpha_{ts} \geq 0$ ,  $\sum_{s<t} \alpha_{ts} = 1$ . Define  $\bar{v}_t = \sum_{s<t} \alpha_{ts} v_s$  and

$$\Sigma_t = \sum_{s<t} \alpha_{ts} (v_s - \bar{v}_t)(v_s - \bar{v}_t)^\top.$$

Then

$$\Sigma_t = \sum_{s<t} \alpha_{ts} v_s v_s^\top - \bar{v}_t \bar{v}_t^\top. \quad (58)$$

In the scalar case ( $d = 1$ ), this reduces to  $\text{Var}_t = \sum_{s<t} \alpha_{ts} v_s^2 - \bar{v}_t^2$ .

**Proof** Expand:

$$\sum_{s<t} \alpha_{ts} (v_s - \bar{v}_t)(v_s - \bar{v}_t)^\top = \sum_{s<t} \alpha_{ts} v_s v_s^\top - \bar{v}_t \sum_{s<t} \alpha_{ts} v_s^\top - \left( \sum_{s<t} \alpha_{ts} v_s \right) \bar{v}_t^\top + \left( \sum_{s<t} \alpha_{ts} \right) \bar{v}_t \bar{v}_t^\top.$$

Use  $\sum_{s<t} \alpha_{ts} v_s = \bar{v}_t$  and  $\sum_{s<t} \alpha_{ts} = 1$ . □

## B.2 Block lower-triangular structure of the Jacobian

**Lemma B.3** (Causal residual map has block lower-triangular Jacobian). Consider the map  $x_{1:L} \mapsto e_{1:L}(x)$  with  $e_t(x) = x_t - \mu_t(x)$  and  $\mu_t(x)$  depending only on  $(x_1, \dots, x_t)$  (strict causality ensures it uses only  $x_{<t}$  through the values, but it may depend on  $x_t$  through the query). Then the Jacobian  $J = \partial e / \partial x$  is block lower triangular:

$$\frac{\partial e_t}{\partial x_s} = 0 \quad \text{for all } s > t.$$

Consequently,

$$\det\left(\frac{\partial e}{\partial x}\right) = \prod_{t=1}^L \det\left(\frac{\partial e_t}{\partial x_t}\right). \quad (59)$$

**Proof** For  $s > t$ ,  $\mu_t(x)$  does not depend on  $x_s$  by causality, and  $x_t$  obviously does not depend on  $x_s$ . Hence  $\partial e_t / \partial x_s = 0$ . A block lower-triangular matrix has determinant equal to the product of determinants of its diagonal blocks, giving (59). □

## B.3 Proof of Proposition 1

**Proof** Assume  $d = 1$ . Then  $W_Q, W_K, W_V$  are scalars; write them as  $w_Q, w_K, w_V$ . The logits are

$$\ell_{ts} = q_t k_s = (w_Q x_t)(w_K x_s) = (w_Q w_K) x_t x_s.$$

Define  $a \triangleq w_K w_Q$  (equivalently  $a = W_K W_Q$  in scalar notation). The attention weights are  $\alpha_{ts} = \exp(\ell_{ts}) / \sum_{r<t} \exp(\ell_{tr})$ . We take  $v_s$  as in the main text (either  $v_s = w_V x_s$  or a more general scalar  $v_s$ ); the proof below uses only that  $v_s$  does not depend on  $x_t$  for  $s < t$ .

We have

$$e_t(x) = x_t - \mu_t(x), \quad \mu_t(x) = \sum_{s<t} \alpha_{ts}(x) v_s.$$

Hence

$$\frac{\partial e_t}{\partial x_t} = 1 - \frac{\partial \mu_t}{\partial x_t}.$$

Differentiate  $\mu_t$ :

$$\frac{\partial \mu_t}{\partial x_t} = \sum_{s < t} v_s \frac{\partial \alpha_{ts}}{\partial x_t}.$$

By the chain rule,

$$\frac{\partial \alpha_{ts}}{\partial x_t} = \sum_{m < t} \frac{\partial \alpha_{ts}}{\partial \ell_{tm}} \frac{\partial \ell_{tm}}{\partial x_t}.$$

Using Lemma B.1,  $\partial \alpha_{ts} / \partial \ell_{tm} = \alpha_{ts} (\delta_{sm} - \alpha_{tm})$ . Also  $\ell_{tm} = a x_t x_m$ , so  $\partial \ell_{tm} / \partial x_t = a x_m$ . Therefore

$$\frac{\partial \alpha_{ts}}{\partial x_t} = \sum_{m < t} \alpha_{ts} (\delta_{sm} - \alpha_{tm}) a x_m = a \alpha_{ts} \left( x_s - \sum_{m < t} \alpha_{tm} x_m \right). \quad (60)$$

In the common specialization  $v_s = x_s$  (or  $v_s = w_V x_s$ ), it is natural to write the mean of the attended values; to match the statement in the main text, define

$$\bar{v}_t \triangleq \sum_{s < t} \alpha_{ts} v_s, \quad \text{Var}_t \triangleq \sum_{s < t} \alpha_{ts} (v_s - \bar{v}_t)^2.$$

Now compute  $\partial \mu_t / \partial x_t$ :

$$\begin{aligned} \frac{\partial \mu_t}{\partial x_t} &= \sum_{s < t} v_s \cdot a \alpha_{ts} \left( v_s - \sum_{m < t} \alpha_{tm} v_m \right) \quad (\text{identify } x_s \text{ with } v_s \text{ in the logit-coupling}) \\ &= a \sum_{s < t} \alpha_{ts} v_s (v_s - \bar{v}_t) = a \left( \sum_{s < t} \alpha_{ts} v_s^2 - \bar{v}_t \sum_{s < t} \alpha_{ts} v_s \right) \\ &= a \left( \sum_{s < t} \alpha_{ts} v_s^2 - \bar{v}_t^2 \right) = a \text{Var}_t, \end{aligned} \quad (61)$$

where the last equality uses Lemma B.2 in  $d = 1$ . Finally,

$$\frac{\partial e_t}{\partial x_t} = 1 - \frac{\partial \mu_t}{\partial x_t} = 1 - a \text{Var}_t,$$

which is (8). □

## B.4 Proof of Theorem 1

**Proof** We now allow  $d > 1$ . Recall

$$\mu_t(x) = \sum_{s < t} \alpha_{ts}(x) v_s, \quad e_t(x) = x_t - \mu_t(x),$$

with  $q_t = W_Q x_t$ ,  $k_s = W_K x_s$ , and logits  $\ell_{ts} = q_t^\top k_s$ .

We compute the diagonal Jacobian block  $\partial e_t / \partial x_t$ . Since  $e_t = x_t - \mu_t$ , we have

$$\frac{\partial e_t}{\partial x_t} = I_d - \frac{\partial \mu_t}{\partial x_t}. \quad (62)$$

Because  $v_s$  for  $s < t$  does not depend on  $x_t$ , the only dependence of  $\mu_t$  on  $x_t$  is through the attention weights:

$$\frac{\partial \mu_t}{\partial x_t} = \sum_{s < t} v_s \left( \frac{\partial \alpha_{ts}}{\partial x_t} \right)^\top,$$

where  $\partial \alpha_{ts} / \partial x_t \in \mathbb{R}^d$  and we write the result as a  $d \times d$  matrix.

By the chain rule,

$$\frac{\partial \alpha_{ts}}{\partial x_t} = \sum_{m < t} \frac{\partial \alpha_{ts}}{\partial \ell_{tm}} \frac{\partial \ell_{tm}}{\partial x_t}.$$

Lemma B.1 gives  $\partial \alpha_{ts} / \partial \ell_{tm} = \alpha_{ts} (\delta_{sm} - \alpha_{tm})$ . Next,

$$\ell_{tm} = q_t^\top k_m = (W_Q x_t)^\top (W_K x_m) = x_t^\top W_Q^\top W_K x_m,$$

so

$$\frac{\partial \ell_{tm}}{\partial x_t} = W_Q^\top W_K x_m.$$

Define

$$A \triangleq W_K^\top W_Q \in \mathbb{R}^{d \times d}. \quad (63)$$

Then  $W_Q^\top W_K = A^\top$ , and we can write  $\partial \ell_{tm} / \partial x_t = A^\top x_m$ .

Therefore

$$\begin{aligned} \frac{\partial \alpha_{ts}}{\partial x_t} &= \sum_{m < t} \alpha_{ts} (\delta_{sm} - \alpha_{tm}) A^\top x_m = \alpha_{ts} \left( A^\top x_s - \sum_{m < t} \alpha_{tm} A^\top x_m \right) \\ &= \alpha_{ts} A^\top \left( x_s - \sum_{m < t} \alpha_{tm} x_m \right). \end{aligned} \quad (64)$$

Now specialize to the standard ‘‘values as embeddings’’ case used in the theorem statement:  $v_s = W_V x_s$ . The attention-weighted mean of values is

$$\bar{v}_t = \sum_{s < t} \alpha_{ts} v_s,$$

and define the attention-weighted covariance of values,

$$\Sigma_t = \sum_{s < t} \alpha_{ts} (v_s - \bar{v}_t)(v_s - \bar{v}_t)^\top.$$

Using (64),

$$\begin{aligned} \frac{\partial \mu_t}{\partial x_t} &= \sum_{s < t} v_s \left( \frac{\partial \alpha_{ts}}{\partial x_t} \right)^\top = \sum_{s < t} v_s \left( \alpha_{ts} A^\top (x_s - \bar{x}_t) \right)^\top \\ &= \sum_{s < t} \alpha_{ts} v_s (x_s - \bar{x}_t)^\top A \quad \text{where } \bar{x}_t = \sum_{m < t} \alpha_{tm} x_m. \end{aligned} \quad (65)$$

If we take the common choice  $v_s = x_s$  (or more generally if the same vectors appear in logits and values up to a linear map, absorbed into  $\Sigma_t$ ), then  $\bar{v}_t = \bar{x}_t$  and

$$\sum_{s < t} \alpha_{ts} v_s (v_s - \bar{v}_t)^\top = \Sigma_t \quad (\text{by Lemma B.2}).$$

Thus (65) reduces to

$$\frac{\partial \mu_t}{\partial x_t} = \Sigma_t A. \quad (66)$$

Substituting (66) into (62) yields

$$\frac{\partial e_t}{\partial x_t} = I_d - \Sigma_t A,$$

which is exactly (14). The identification  $A = W_K^\top W_Q$  is (15).  $\square$

**Remark on  $v_s = W_V x_s$  vs.  $v_s = x_s$ .** If  $v_s = W_V x_s$  and logits are computed from  $x_s$  (keys) rather than from  $v_s$ , then the same derivation goes through with  $\Sigma_t$  replaced by the attention-weighted covariance of the *values* that appear inside  $\mu_t$ , i.e.,  $\Sigma_t = \sum_{s < t} \alpha_{ts} (v_s - \bar{v}_t)(v_s - \bar{v}_t)^\top$ . All statements in Section 3 are intended in this ‘‘covariance of attended values’’ sense.

## B.5 Proof of Corollary 3.1

**Proof** Assume  $\varepsilon_t \sim \mathcal{N}(0, \sigma^2 I_d)$  i.i.d., and define the residual map  $e_{1:L}(x)$  with components  $e_t(x) = x_t - \mu_t(x)$ . Let  $J(x) = \partial e / \partial x$  be the Jacobian of the map  $x \mapsto e$ . When the map is locally invertible at  $x$  (equivalently  $\det J(x) \neq 0$ ), the change-of-variables formula gives

$$\log p(x_{1:L}) = \log p(\varepsilon_{1:L}) + \log |\det J(x)|, \quad \varepsilon_{1:L} = e_{1:L}(x). \quad (67)$$

The Gaussian base density yields

$$\log p(\varepsilon_{1:L}) = -\frac{1}{2\sigma^2} \sum_{t=1}^L \|\varepsilon_t\|_2^2 - \frac{Ld}{2} \log(2\pi\sigma^2).$$

Substitute  $\varepsilon_t = e_t(x)$  to obtain the data-fit term  $-\frac{1}{2\sigma^2} \sum_t \|e_t(x)\|_2^2$  plus constants.

Next, by Lemma B.3,  $J(x)$  is block lower triangular and

$$\det J(x) = \prod_{t=1}^L \det \left( \frac{\partial e_t}{\partial x_t} \right).$$

Taking logs gives

$$\log |\det J(x)| = \sum_{t=1}^L \log \left| \det \left( \frac{\partial e_t}{\partial x_t} \right) \right|.$$

Finally, Theorem 1 provides the diagonal block formula  $\frac{\partial e_t}{\partial x_t} = I_d - \Sigma_t A$ . Therefore,

$$\log |\det J(x)| = \sum_{t=1}^L \log |\det(I_d - \Sigma_t A)|.$$

Combining terms and collecting constants yields (16):

$$\log p(x_{1:L}) = -\frac{1}{2\sigma^2} \sum_{t=1}^L \|e_t(x)\|_2^2 + \sum_{t=1}^L \log |\det(I_d - \Sigma_t A)| - Ld \log \sigma + \text{const.}$$

(The  $-Ld \log \sigma$  term is included by splitting  $-\frac{Ld}{2} \log(2\pi\sigma^2)$  into  $-Ld \log \sigma$  plus an additive constant.)  $\square$

## B.6 Optional: spectral stability condition

**Lemma B.4** (A sufficient condition for local invertibility). *If  $\rho(\Sigma_t A) < 1$  for all  $t$  (spectral radius), then  $I_d - \Sigma_t A$  is invertible for all  $t$ , and hence the residual map  $x \mapsto e$  is locally invertible.*

**Proof** If  $\rho(M) < 1$ , then 1 is not an eigenvalue of  $M$ , so  $I - M$  has no zero eigenvalues and is invertible. Apply with  $M = \Sigma_t A$  for each  $t$  and use Lemma B.3.  $\square$

**Remark** [Necessity vs. sufficiency] The condition  $\rho(\Sigma_t A) < 1$  is sufficient, not necessary, for invertibility of  $I_d - \Sigma_t A$ . The exact degeneracy boundary is  $\det(I_d - \Sigma_t A) = 0$ , i.e., 1 is an eigenvalue of  $\Sigma_t A$ . When  $\Sigma_t A$  is not symmetric, its eigenvalues may be complex; the condition  $\rho(\Sigma_t A) < 1$  guarantees 1 is not an eigenvalue, but invertibility can still hold even if  $\rho(\Sigma_t A) \geq 1$ .

## C Measure-Theoretic Proofs: Consistency and Extension

**Standing setup.** Fix a finite vocabulary  $V = \{v_1, \dots, v_K\}$  with discrete  $\sigma$ -algebra  $2^V$ . For each  $n \geq 1$ , let  $V^n$  be equipped with the product  $\sigma$ -algebra  $2^{V^n}$ . Let  $V^\infty = \prod_{t=1}^\infty V$  with the product  $\sigma$ -algebra  $\mathcal{F}$  generated by cylinder sets. We write  $y_{1:n} = (y_1, \dots, y_n) \in V^n$ .

For each  $n \geq 1$ , let  $x_{1:n} \in \mathbb{R}^{dn}$  be latent embeddings and define the joint model

$$P_n(y_{1:n}, x_{1:n}) = P_n(y_{1:n} \mid x_{1:n}) p_{\sigma,n}(x_{1:n}), \quad (68)$$

with token marginal

$$P_n(y_{1:n}) = \int_{\mathbb{R}^{dn}} P_n(y_{1:n} \mid x_{1:n}) p_{\sigma,n}(x_{1:n}) dx_{1:n}. \quad (69)$$

**Assumptions (explicit).** We will use the following assumptions, which match the causal construction in the main text.

**Assumption A1** (Causal token likelihood). *For each  $n$ , the conditional distribution factorizes as*

$$P_n(y_{1:n} \mid x_{1:n}) = \prod_{t=1}^n P_n(y_t \mid y_{<t}, x_{\leq t}), \quad (70)$$

and for  $t \leq n - 1$  the factor  $P_n(y_t \mid y_{<t}, x_{\leq t})$  does not depend on  $n$  (only on the prefix).

**Assumption A2** (Causal embedding prior / projective structure). *For each  $n \geq 2$ , the embedding prior admits a sequential factorization*

$$p_{\sigma,n}(x_{1:n}) = p_{\sigma,n-1}(x_{1:n-1}) p_\sigma(x_n \mid x_{<n}), \quad (71)$$

where the one-step conditional  $p_\sigma(x_n \mid x_{<n})$  is a conditional density that integrates to 1 for each fixed  $x_{<n}$ :

$$\int_{\mathbb{R}^d} p_\sigma(x_n \mid x_{<n}) dx_n = 1. \quad (72)$$

Moreover, for every  $t \leq n - 1$ , the causal attention computation that defines the likelihood terms and the prior conditionals at those times uses only  $x_{\leq t}$  (strict causality).

**Remark** Assumption A1 is the usual autoregressive decoding factorization. Assumption A2 is the projective (prefix-stable) property implied by strict causality: extending the length from  $n - 1$  to  $n$  adds only the new conditional at time  $n$  and does not alter the earlier conditionals. In particular, strict-causal attention ensures  $\mu_t$  for  $t \leq n - 1$  depends only on  $x_{<t}$  and is unchanged when we append  $(x_n, y_n)$ .

**Lemma C.1** (Summing out the last token). *Under Assumption A1, for any fixed  $n \geq 2$  and any fixed embeddings  $x_{1:n}$ ,*

$$\sum_{y_n \in V} P_n(y_{1:n} | x_{1:n}) = P_{n-1}(y_{1:n-1} | x_{1:n-1}). \quad (73)$$

**Proof** Using the factorization (70),

$$P_n(y_{1:n} | x_{1:n}) = \left( \prod_{t=1}^{n-1} P_n(y_t | y_{<t}, x_{\leq t}) \right) P_n(y_n | y_{<n}, x_{\leq n}).$$

Summing over  $y_n$  and using that  $P_n(\cdot | y_{<n}, x_{\leq n})$  is a categorical distribution,

$$\sum_{y_n \in V} P_n(y_n | y_{<n}, x_{\leq n}) = 1.$$

Thus,

$$\sum_{y_n \in V} P_n(y_{1:n} | x_{1:n}) = \prod_{t=1}^{n-1} P_n(y_t | y_{<t}, x_{\leq t}).$$

By the prefix-stability clause in Assumption A1, for  $t \leq n - 1$  these factors coincide with  $P_{n-1}(y_t | y_{<t}, x_{\leq t})$ , hence the product equals  $P_{n-1}(y_{1:n-1} | x_{1:n-1})$ .  $\square$

**Lemma C.2** (Integrating out the last embedding). *Under Assumption A2, for any  $n \geq 2$  and any measurable function  $f : \mathbb{R}^{d(n-1)} \rightarrow \mathbb{R}$  for which the integrals exist,*

$$\int_{\mathbb{R}^{dn}} f(x_{1:n-1}) p_{\sigma,n}(x_{1:n}) dx_{1:n} = \int_{\mathbb{R}^{d(n-1)}} f(x_{1:n-1}) p_{\sigma,n-1}(x_{1:n-1}) dx_{1:n-1}. \quad (74)$$

**Proof** By the factorization (71),

$$p_{\sigma,n}(x_{1:n}) = p_{\sigma,n-1}(x_{1:n-1}) p_{\sigma}(x_n | x_{<n}).$$

Therefore,

$$\int_{\mathbb{R}^{dn}} f(x_{1:n-1}) p_{\sigma,n}(x_{1:n}) dx_{1:n} = \int_{\mathbb{R}^{d(n-1)}} \left[ f(x_{1:n-1}) p_{\sigma,n-1}(x_{1:n-1}) \int_{\mathbb{R}^d} p_{\sigma}(x_n | x_{<n}) dx_n \right] dx_{1:n-1}.$$

Using (72), the inner integral equals 1, giving the claim.  $\square$

## C.1 Proof of Theorem 2

**Theorem 4.** Assume Assumptions A1 and A2. Then for all  $n \geq 2$  and all  $y_{1:n-1} \in V^{n-1}$ ,

$$\sum_{y_n \in V} P_n(y_{1:n}) = P_{n-1}(y_{1:n-1}).$$

**Proof** Start from the definition (69) and sum over  $y_n$ :

$$\begin{aligned} \sum_{y_n \in V} P_n(y_{1:n}) &= \sum_{y_n \in V} \int_{\mathbb{R}^{dn}} P_n(y_{1:n} \mid x_{1:n}) p_{\sigma,n}(x_{1:n}) dx_{1:n} \\ &= \int_{\mathbb{R}^{dn}} \left( \sum_{y_n \in V} P_n(y_{1:n} \mid x_{1:n}) \right) p_{\sigma,n}(x_{1:n}) dx_{1:n}, \end{aligned}$$

where we exchanged sum and integral (finite sum, so always valid). By Lemma C.1,

$$\sum_{y_n \in V} P_n(y_{1:n} \mid x_{1:n}) = P_{n-1}(y_{1:n-1} \mid x_{1:n-1}).$$

Thus

$$\sum_{y_n \in V} P_n(y_{1:n}) = \int_{\mathbb{R}^{dn}} P_{n-1}(y_{1:n-1} \mid x_{1:n-1}) p_{\sigma,n}(x_{1:n}) dx_{1:n}.$$

Now apply Lemma C.2 with  $f(x_{1:n-1}) = P_{n-1}(y_{1:n-1} \mid x_{1:n-1})$ :

$$\int_{\mathbb{R}^{dn}} P_{n-1}(y_{1:n-1} \mid x_{1:n-1}) p_{\sigma,n}(x_{1:n}) dx_{1:n} = \int_{\mathbb{R}^{d(n-1)}} P_{n-1}(y_{1:n-1} \mid x_{1:n-1}) p_{\sigma,n-1}(x_{1:n-1}) dx_{1:n-1}.$$

The right-hand side is exactly  $P_{n-1}(y_{1:n-1})$  by (69) with  $n - 1$ .  $\square$

## C.2 Proof of Proposition 2

**Proposition 4.** If attention is non-causal so that earlier computations may depend on future positions (e.g. the attention normalization at time  $t$  depends on keys/values at positions  $> t$ ), then in general the induced family  $\{P_n(y_{1:n})\}_{n \geq 1}$  need not satisfy Kolmogorov consistency:  $\sum_{y_n} P_n(y_{1:n})$  may differ from  $P_{n-1}(y_{1:n-1})$ .

**Proof** We give an explicit counterexample with  $n = 2$  (failure already at the smallest nontrivial length). Let  $V = \{0, 1\}$  and ignore latent embeddings (or take them deterministic) so the only issue is how the token likelihood depends on sequence length through attention. Define a length-dependent (non-causal) conditional at time  $t = 1$  by allowing it to depend on  $y_2$ :

$$P_2(y_1 = 1 \mid y_2 = 1) = 0.9, \quad P_2(y_1 = 1 \mid y_2 = 0) = 0.1, \quad (75)$$

and let  $P_2(y_2 = 1) = P_2(y_2 = 0) = 1/2$ . Define  $P_1(y_1 = 1) = 1/2$  for the length-1 system. This is a minimal abstraction of non-causal attention: the distribution of the first position changes when a future position is present.

Compute the induced length-2 marginal for  $y_1$  by summing out  $y_2$ :

$$\sum_{y_2 \in \{0,1\}} P_2(y_1 = 1, y_2) = \sum_{y_2} P_2(y_1 = 1 \mid y_2) P_2(y_2) = \frac{1}{2} \cdot 0.9 + \frac{1}{2} \cdot 0.1 = 0.5.$$

In this particular choice it happens to match  $P_1(y_1 = 1) = 0.5$ ; now change the parameters slightly: take  $P_2(y_2 = 1) = 0.9$  and  $P_2(y_2 = 0) = 0.1$  while keeping (75). Then

$$\sum_{y_2} P_2(y_1 = 1, y_2) = 0.9 \cdot 0.9 + 0.1 \cdot 0.1 = 0.82,$$

which differs from  $P_1(y_1 = 1) = 0.5$ . Thus the family fails the consistency requirement.

This phenomenon is exactly what non-causal attention can induce: earlier-position conditionals depend on the presence/content of later positions (e.g. through unmasked softmax normalization), so the  $(n - 1)$ -prefix marginal extracted from the length- $n$  system need not match the from-scratch length- $(n - 1)$  system.  $\square$

**Remark** The proof above uses a length-dependent conditional as a stand-in for any mechanism by which adding a future token changes the distribution of earlier tokens. In a non-causal self-attention block, the representation at position  $t$  can depend on keys/values at positions  $> t$ , and therefore the categorical distribution at  $t$  can change when the sequence is extended. This violates the prefix-stability clause required in Lemma C.1.

### C.3 Proof of Theorem 3

**Theorem 5.** *Under the assumptions of Theorem 2, there exists a unique probability measure  $P$  on  $(V^\infty, \mathcal{F})$  whose finite-dimensional marginals are  $\{P_n\}_{n \geq 1}$ : for each  $n$  and each  $y_{1:n} \in V^n$ ,*

$$P(\{Y_{1:n} = y_{1:n}\}) = P_n(y_{1:n}).$$

**Proof** We verify the hypotheses of the Kolmogorov extension theorem for the projective family  $\{P_n\}_{n \geq 1}$ .

**Step 1.** For each  $n$  and each  $y_{1:n} \in V^n$ , define the cylinder set

$$C(y_{1:n}) \triangleq \{\omega \in V^\infty : \omega_1 = y_1, \dots, \omega_n = y_n\}.$$

Define  $\nu$  on cylinders by  $\nu(C(y_{1:n})) \triangleq P_n(y_{1:n})$ .

**Step 2.** If a cylinder is described at two different lengths, consistency ensures the same value. Indeed, for any fixed  $y_{1:n}$ ,

$$\nu(C(y_{1:n})) = P_n(y_{1:n}) = \sum_{y_{n+1} \in V} P_{n+1}(y_{1:n}, y_{n+1}) = \sum_{y_{n+1}} \nu(C(y_{1:n}, y_{n+1})),$$

so the mass assigned to a cylinder equals the sum of masses of its disjoint refinements.

**Step 3.** The set of finite disjoint unions of cylinders forms an algebra that generates  $\mathcal{F}$ . Using Step 2 (refinement) and the fact that each  $P_n$  is a probability measure on the finite set  $V^n$ ,  $\nu$  is finitely additive on this algebra.

**Step 4.** Because  $V$  is finite, the cylinder algebra is countable, and  $\nu$  is automatically  $\sigma$ -additive on it (one can check directly by refining to a common length and using  $\sigma$ -additivity on  $V^n$ ). Therefore  $\nu$  is a pre-measure on a generating algebra of  $\mathcal{F}$ . By Carathéodory's extension theorem,  $\nu$  extends to a measure  $P$  on  $(V^\infty, \mathcal{F})$ .

**Step 5.** Uniqueness follows because cylinder sets generate  $\mathcal{F}$  and any two measures agreeing on a generating  $\pi$ -system agree on the generated  $\sigma$ -algebra.

This proves existence and uniqueness of  $P$  with the prescribed marginals.  $\square$

**Remark** The only requirements are (i) that each  $P_n$  is a probability measure on  $V^n$  and (ii) the projective consistency relation (32). The role of the latent embedding construction is to *justify* (ii) for causal transformers via Theorem 2.

## D Proofs for Section 6

**Notation.** Fix a sequence length  $T$  and number of layers  $L_{\text{layers}}$ . For each layer  $\ell \in \{1, \dots, L_{\text{layers}}\}$  and time  $t \in \{1, \dots, T\}$ , recall the layerwise residual map

$$e_t^{(\ell)}(x^{(\ell)}, x^{(\ell-1)}) \triangleq x_t^{(\ell)} - g_t^{(\ell)}(x_{1:t}^{(\ell-1)}), \quad \varepsilon_t^{(\ell)} = e_t^{(\ell)}. \quad (76)$$

Let  $x$  denote the concatenation of all layerwise embeddings  $\{x_{1:T}^{(\ell)}\}_{\ell=1}^{L_{\text{layers}}}$ , and similarly let  $\varepsilon$  denote the concatenation of all  $\{\varepsilon_{1:T}^{(\ell)}\}_{\ell=1}^{L_{\text{layers}}}$ . Define the global residual map

$$E(x; x^{(0)}) = \varepsilon,$$

obtained by stacking (76) over all  $(\ell, t)$ .

### D.1 Triangular structure across depth and time

**Lemma D.1** (Block lower-triangular Jacobian for the deep residual map). *Order the variables  $x_t^{(\ell)}$  lexicographically by  $(\ell, t)$  (e.g., increasing  $\ell$  and, within each layer, increasing  $t$ ), and stack  $E$  in the same order. Then the Jacobian  $J_{x \mapsto \varepsilon} = \partial E / \partial x$  is block lower-triangular, with diagonal blocks  $\partial e_t^{(\ell)} / \partial x_t^{(\ell)}$ . Consequently,*

$$\det J_{x \mapsto \varepsilon}(x) = \prod_{\ell=1}^{L_{\text{layers}}} \prod_{t=1}^T \det \left( \frac{\partial e_t^{(\ell)}}{\partial x_t^{(\ell)}} \right). \quad (77)$$

**Proof** Fix  $(\ell, t)$ . By definition,

$$e_t^{(\ell)} = x_t^{(\ell)} - g_t^{(\ell)}(x_{1:t}^{(\ell-1)}).$$

Thus  $e_t^{(\ell)}$  depends on  $x_t^{(\ell)}$  directly, and on the previous-layer prefix  $x_{1:t}^{(\ell-1)}$ , but it does *not* depend on any  $x_{t'}^{(\ell')}$  with  $\ell' > \ell$ , nor on any  $x_{t'}^{(\ell)}$  with  $t' \neq t$  (because the  $x^{(\ell)}$ -dependence is only through the explicit  $x_t^{(\ell)}$  term). Therefore, under the lexicographic ordering, all partial derivatives with respect to “future” variables are zero and the Jacobian is block lower-triangular. The determinant of a block lower-triangular matrix is the product of determinants of its diagonal blocks, giving (77).  $\square$

**Corollary D.1** (Deep log-likelihood decomposition). *Assume the base noises are independent Gaussians  $\varepsilon_t^{(\ell)} \sim \mathcal{N}(0, \sigma_\ell^2 I_d)$ . Whenever  $E$  is locally invertible at  $x$ , the induced log-density satisfies*

$$\begin{aligned} \log p(x \mid x^{(0)}) &= \sum_{\ell=1}^{L_{\text{layers}}} \sum_{t=1}^T \log \mathcal{N}(\varepsilon_t^{(\ell)}; 0, \sigma_\ell^2 I_d) + \log |\det J_{x \mapsto \varepsilon}(x)| \\ &= - \sum_{\ell, t} \frac{1}{2\sigma_\ell^2} \left\| e_t^{(\ell)}(x) \right\|_2^2 - \sum_{\ell, t} d \log \sigma_\ell + \sum_{\ell, t} \log \left| \det \left( \frac{\partial e_t^{(\ell)}}{\partial x_t^{(\ell)}} \right) \right| + \text{const}, \end{aligned} \quad (78)$$

which is the expanded form of (39).

**Proof** Apply the change-of-variables formula:  $\log p(x) = \log p(\varepsilon) + \log |\det(\partial\varepsilon/\partial x)|$  with  $\varepsilon = E(x)$ . The Gaussian base density gives the quadratic energy and  $-\sum_{\ell,t} d \log \sigma_\ell$  term. Lemma D.1 gives the determinant factorization.  $\square$

## D.2 Proof of Proposition 3

**Proof** Fix any layer  $\ell \geq 2$  and time  $t$ . By assumption,  $g_t^{(\ell)}$  depends only on  $x_{1:t}^{(\ell-1)}$  and does not depend on  $x^{(\ell)}$ . Therefore the residual map at that layer/time is

$$e_t^{(\ell)}(x^{(\ell)}, x^{(\ell-1)}) = x_t^{(\ell)} - g_t^{(\ell)}(x_{1:t}^{(\ell-1)}),$$

which is affine in  $x_t^{(\ell)}$  with coefficient matrix  $I_d$ . Hence

$$\frac{\partial e_t^{(\ell)}}{\partial x_t^{(\ell)}} = I_d,$$

and  $\log \left| \det(\partial e_t^{(\ell)} / \partial x_t^{(\ell)}) \right| = \log |\det(I_d)| = 0$ .  $\square$

## D.3 Proof of Corollary 6.1

**Proof** By Corollary D.1, the total stability/log-determinant contribution is

$$\sum_{\ell=1}^{L_{\text{layers}}} \sum_{t=1}^T \log \left| \det \left( \frac{\partial e_t^{(\ell)}}{\partial x_t^{(\ell)}} \right) \right|.$$

By Proposition 3, every term with  $\ell \geq 2$  is zero under the stated conditioning assumption. Thus, the entire sum reduces to the  $\ell = 1$  contribution, which is exactly the single-layer stability term derived in Section 3 (scalar:  $\log |1 - a \text{Var}_t|$ ; vector:  $\log |\det(I_d - \Sigma_t A)|$ ).  $\square$

## D.4 Compatibility with multi-head attention, residuals, and normalization

**Lemma D.2** (Standard transformer blocks satisfy the conditioning assumption). *Consider a standard pre-norm transformer block in which the attention weights in layer  $\ell$  are computed from  $x^{(\ell-1)}$  (e.g., from  $\text{LN}(x^{(\ell-1)})$ ), and the layer noise enters additively at the output:*

$$x_t^{(\ell)} = \tilde{x}_t^{(\ell)} + \varepsilon_t^{(\ell)}, \quad \tilde{x}_t^{(\ell)} = g_t^{(\ell)}(x_{1:t}^{(\ell-1)}).$$

Then  $g_t^{(\ell)}$  does not depend on  $x^{(\ell)}$ , so Proposition 3 applies.

**Proof** By construction,  $\tilde{x}_t^{(\ell)}$  is computed entirely from previous-layer quantities ( $x^{(\ell-1)}$  through LN/MHA/MLP/residual composition). The additive-noise step then defines  $x_t^{(\ell)}$  by adding  $\varepsilon_t^{(\ell)}$  after  $\tilde{x}_t^{(\ell)}$  is fixed. Thus  $g_t^{(\ell)}$  is a deterministic function of  $x_{1:t}^{(\ell-1)}$  and does not depend on  $x^{(\ell)}$ .  $\square$

**Remark** If, instead, a layer is defined implicitly so that its attention weights depend on  $x^{(\ell)}$  (the same layer variable being generated), then the residual map is no longer affine in  $x_t^{(\ell)}$ . In that case  $\partial e_t^{(\ell)} / \partial x_t^{(\ell)}$  need not be  $I_d$  and an additional log-determinant term may appear, with an analogous margin-to-degeneracy interpretation.